

RESISTIVITY SURVEY OF THE CISOLOK-CISUKARAME  
GEOTHERMAL AREA, WEST JAVA, INDONESIA

Idrus Alhamid\*  
UNU Geothermal Training Programme  
National Energy Authority  
Grensasvegur 9, 108 Reykjavik  
ICELAND

\*

Permanent address:  
PERTAMINA  
Exploration and Production Directorate  
Geothermal Division  
Head Office, P.O. Box 12, Jakarta  
INDONESIA

ABSTRACT

The first part of this report gives a brief discussion concerning the basic principle, field technique, instrumentation and interpretation of the DC-resistivity measurement. The second part deals with the geology, geochemistry and geophysical study of the Cisolok-Cisukarame geothermal area, West Java, with the main emphasis on DC Schlumberger Sounding measurement done in 1976 and 1982. About 76 Schlumberger Sounding data were analyzed and interpreted with one-dimensional modelling and several cross-sections were made to understand the resistivity layers of the area. Two-dimensional interpretation was also applied using 10 soundings measured along D-line in Cisukarame Area. Both interpretations gave similar results, that there is a possibility of the existing of a geothermal reservoir in the Cisukarame Area. From the geothermometer calculations done in Iceland an underground temperature was estimated in the range of 150-175 °C for Cisukarame but only 110-150 °C for the Cisolok Area. In spite of the results obtained by the resistivity measurements this underground temperature does not show a very promising temperature for hot water to flush into steam at depths.

TABLE OF CONTENTS

	Page
ABSTRACT .....	3
1 INTRODUCTION	
1.1 Scope of work .....	9
2 RESISTIVITY MEASUREMENTS IN GEOTHERMAL EXPLORATION	
2.1 Resistivity of water saturated rocks .....	10
2.1.1 The texture and porosity of the rocks .....	10
2.1.2 The salinity of the water .....	11
2.1.3 The temperature .....	12
2.1.4 Partially saturated rocks .....	13
2.1.5 Water rock interaction .....	15
2.2 The basic theory of DC-resistivity measurements .	16
2.2.1 The Schlumberger array .....	17
2.2.2 The head-on array .....	18
2.2.3 The dipole-dipole arrangement .....	19
2.2.4 The dipole-equatorial arrangement .....	21
2.2.5 The dipole-axial arrangement .....	21
2.3 Field techniques .....	22
2.4 Instrumentation .....	23
2.5 Measurement errors .....	24
2.6 One-dimensional Schlumberger interpretation .....	24
2.7 Two-dimensional interpretation .....	26
3 GEOTHERMAL ACTIVITY IN THE CISOLOK-CISUKARAME AREA	
3.1 Introduction .....	27
3.2 Geological-setting .....	28
3.3 Geothermal surface manifestations .....	30
3.3.1 The Cisukarame area .....	30
3.3.2 The Cisolok area .....	31
3.3.3 The Sangiang area .....	31
3.4 The data quality and interpretation .....	32
3.5 Cisukarame 1-dimensional interpretation .....	33
3.5.1 The Cisukarame area iso-resistivity map .....	37

3.6	Cisukarame 2-dimensional interpretation .....	39
3.7	Cisolok 1-dimensional interpretation .....	39
3.8	Conclusions .....	42
3.9	Recommendations .....	43
ACKNOWLEDGMENTS .....		45
REFERENCES .....		46
APPENDIX I	Resistivity data, 1-dimensional interpretation and calculated curves .....	48
APPENDIX II	Computer output of geothermometer calculations result .....	62

#### LIST OF FIGURES

1.	The relationship between resistivity of a NaCl solution and salinity of an electrolytic solution at different temperatures .....	12
2.	Resistivity of a NaCl solution as a function of temperature for three different concentrations ....	14
3.	Schlumberger array configuration .....	17
4.	The head-on array .....	18
5.	The dipole-dipole array .....	20
6.	The dipole equatorial array .....	21
7.	The dipole axial arrangement .....	22
8.	Changes of $\rho_{aAC}$ and $\rho_{aBC}$ across a fault .....	26
9.	Physiographic schetsmap of Bayah Dome Pelabuhan Ratu, West Java, Indonesia .....	29

10.	Cross-section A, Cisukarame area .....	34
11.	Cross-section B, Cisukarame area .....	34
12.	Cross-section C, Cisukarame area .....	36
13.	Cross-section D, Cisukarame area .....	36
14.	Cross-section E, Cisukarame area .....	36
15.	Isoresistivity map of the Cisukarame area .....	38
16.	2-dimensional interpretation of resistivity soundings, Cisukarame area .....	40
17.	Cross-section A, Cisolok area .....	41
18.	Cross-section B, Cisolok area .....	41

\*B: A geological map of the Cisolok-Cisukarame area showing the location of the resistivity cross sections is in a pocket of the back cover.

## 1 INTRODUCTION

### 1.1 Scope of work

The author of this report was awarded a United Nations University Fellowship to attend the UNU Geothermal Training Programme at The National Energy Authority in Iceland for 6 months training in geophysical exploration in 1982.

An introductory lecture course covering most aspects of geothermal exploration, production and utilization was given in the first month. Thereafter the author attended special lectures and exercises in geophysical measurements (2 weeks) such as gravity, magnetic and resistivity including interpretation of the data using computer programmes.

The author also participated in the measurement of several lines of "Combined Head-On" (half Schlumberger) profiling to detect vertical structures in the Selfoss low temperature geothermal area, and Schlumberger soundings in the Svartsengi high temperature area (2 weeks). The author further participated in a field excursion to most of the geothermal fields in Iceland under exploration and exploitation (high and low temperature) and visited several factories using geothermal energy (2 weeks). For one week the author received training in microearthquake studies (passive seismic method) at the Science Institute of the University of Iceland.

The main research project of the author was the interpretation of Schlumberger soundings data from the Cislok-Cisukarame geothermal area in Java, Indonesia, and the relation of the resistivity to the geology and geochemistry of the area. The data were brought by the author from Indonesia. About ten weeks were spent on learning the interpretation methods and on writing the report.

## 2 RESISTIVITY MEASUREMENTS IN GEOTHERMAL EXPLORATION

### 2.1 Resistivity of water saturated rocks

World wide experience has proved the dc resistivity method to be a very useful tool in the exploration of geothermal. Water dominated geothermal systems usually have a lower resistivity than the surrounding colder rocks, whereas vapour dominated systems may be characterized by high resistivity. The resistivity of rocks is controlled by several parameters; which will be dealt with in the following sections.

#### 2.1.1. The texture and porosity of the rocks

In general dry, coarse grained crystalline rocks have a high resistivity, but fine grained clays, highly vesicular and altered rocks as well as alteration products show a low resistivity. Usually the water has a lower resistivity than the rock matrix itself and is the dominant factor in the resistivity of the rock as a whole. This correlation can be expressed by Archie's Law (Keller and Frischknecht, 1966):

$$\rho = a \cdot \rho_w \cdot \phi^{-m} \quad (1)$$

where:

$\rho$  = the bulk measured resistivity of water saturated rock

$\rho_w$  = the resistivity of water filling the pores;

$\phi$  = the fractional amount of porosity in comparison with the total volume;

$a$  = a constant which is less than 1 for intergranular porosity and higher than 1 for jointporosity;

$m$  = the cementing factor which varies from 1.2 for unconsolidated sediments to 3.5 for crystalline rocks;

As a first approximation the values  $a = 1$  and  $m = 2$  are used.

Equation (1) indicates that the ratio  $\rho/\rho_w$  is constant for a given porosity. This relation can be expressed by the formula:

$$F = a \cdot \phi^{-n} \quad (2)$$

where  $F$  is called the formation factor.

### 2.1.2 The salinity of the water

The salinity of the water (liquid) present in the pore space of the rock affects the resistivity of the bulk rock. We can look upon the water as an electrolyte. The conductivity of an electrolyte solution can be expressed by

$$\sigma = 1/\rho = F(C_1 \cdot m_1 + C_2 \cdot m_2 + C_3 \cdot m_3 \dots) \quad (3)$$

where  $m_1$  = mobility of different ions

$C_1$  = concentration of ions

$F$  = Faraday's number (96500 Coulombs)

The concept of an equivalent salinity is usually used in explaining the resistivity of ground water. The equivalent salinity of a solution is defined as the salinity of a NaCl solution having the same resistivity as a solution containing various salts.

The advantage of using equivalent salinity is that only one table (or graph) for a single salt is needed to determine the resistivity of a solution. The curves showing the relationship between the resistivity and the salinity of NaCl solutions at various temperatures are shown in Fig. 1.



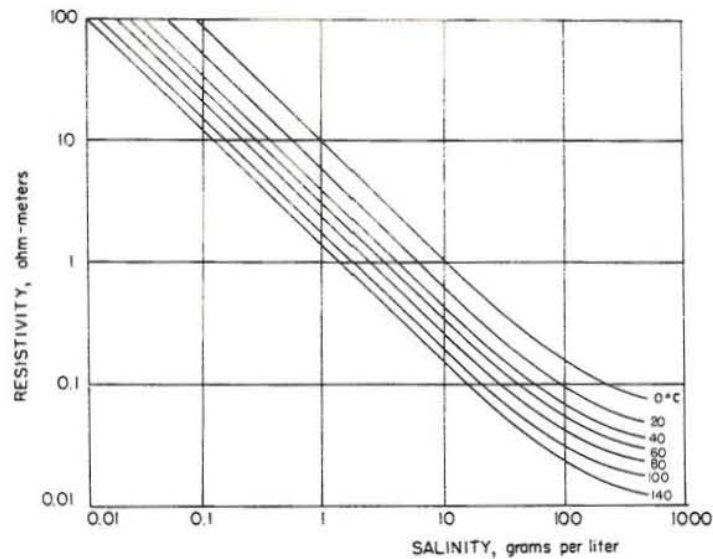


Fig. 1 The relationship between the resistivity of a NaCl solution and the salinity of an electrolytic solution at different temperatures (Keller and Frischknecht, 1966).

This figure shows that there is an almost linear relationship between the salinity and the conductivity of electrolytic solutions. For  $t = 0^{\circ}\text{C}$  the relation between the salinity and the resistivity can be determined by the equation:  $\rho = 0.211 \cdot C - 0.937$  where the resistivity ( $\rho$ ) is in Ohm-meters and  $C$  in mol (1 mol = 58450 ppm)

### 2.1.3 The temperature

By increasing the temperature of the fluid the resistivity of it decreases. This is caused by a lower viscosity and a higher mobility of ions. The relationship between temperature and resistivity of water bearing rocks is sometimes expressed by this equation (Keller and Frischknecht, 1966):

$$\rho_t = \frac{\rho_o}{1 + \alpha (t - t_o)} \quad (4)$$

where:

- $\rho_o$  = the resistivity of the rock at a given reference temperature in ohm-meters;
- $t_o$  = the reference temperature in °C
- $\alpha$  = the temperature coefficient of resistivity, which has a value near 0.025 for most electrolytes.

The influence of the salinity and temperature on resistivity can thus be shown by the formula:

$$\rho_t = \frac{a \cdot \rho_{w_o} \cdot \phi^{-n}}{1 + \alpha (t - t_o)} \quad (5)$$

The formula is valid for temperatures between 0-200°C. At higher temperatures,  $t > 300^\circ\text{C}$  the resistivity tends to increase with the temperature. This is caused by the great decrease in the electric characteristics of water, causing reduction in polarization of the water molecules (see Fig. 2).

#### 2.1.4 Partially saturated rocks

The bulk conductivity of a water bearing rock is reduced if the rocks are partially filled with electrolyte and the rest by oil, air or steam (Keller and Frischknecht, 1966). This relationship is shown by:

$$\rho = \rho_o * S_w^{-n} \quad ; \quad S_w > S_{wc} \quad (6)$$

where

- $\rho$  = is the bulk resistivity of a partially saturated rock

$\rho_o$  = the resistivity of the same rock if it is saturated

$S_w$  = is the fraction of the total pore volume filled with eletrolyte

$n$  = a parameter which is determined experimentally and has a value of approximately 2

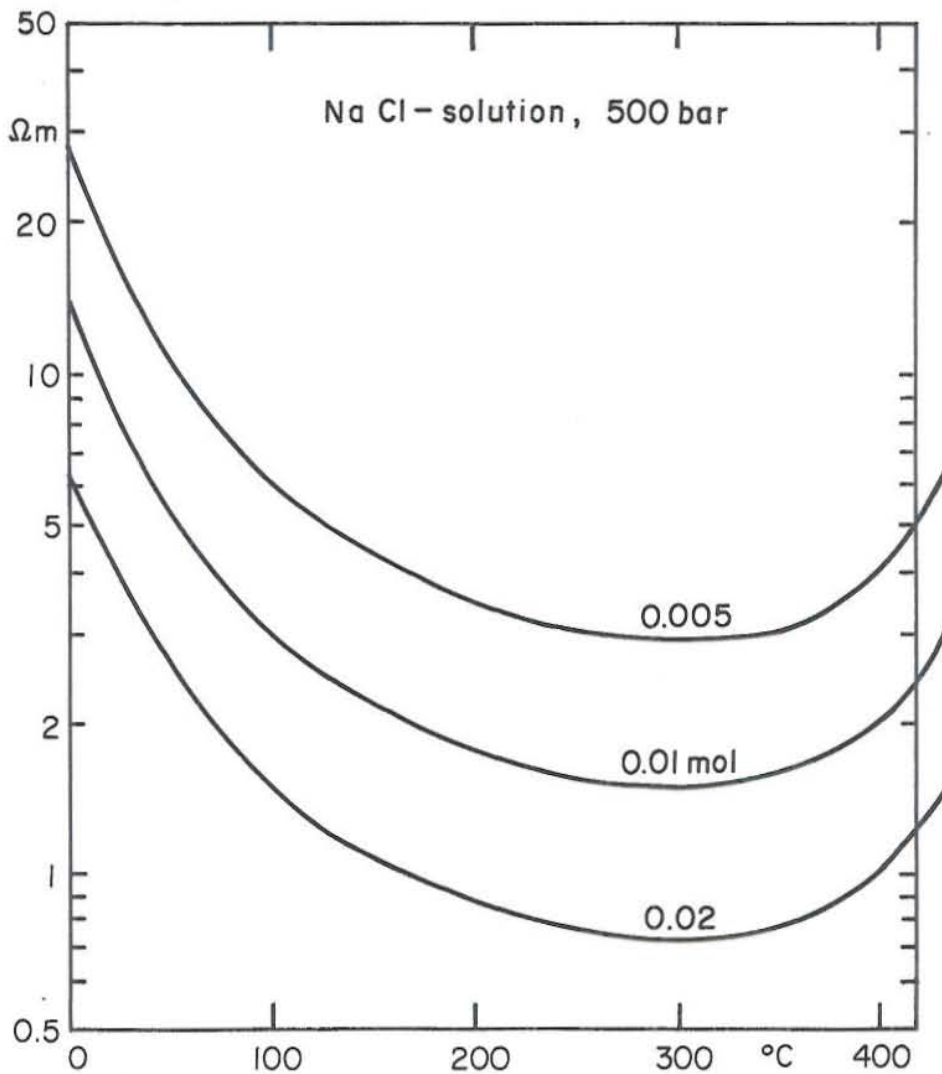


Fig. 2. Resistivity of NaCl solution as a function of temperature for three different concentrations (Quist and Marshall, 1968).

Equation (6) is valid when the water content is greater than some critical value,  $S_{wc}$  which depends on the texture of the rock.

At saturation below the critical saturation the following formula is used:

$$\rho = \rho_o \cdot a \cdot S_w^{-n_2} \quad S_w < S_{wc} \quad (7)$$

where  $a$  and  $n_2$  are parameters determined experimentally;  $a$  varies from 0.05 for sandstone to about 0.5 for igneous rocks and  $n_2$  has a value between 4 and 5.

The critical water saturation is about 25% of the total pore space for sandstone and similar permeable rocks, but may be as large as 70 to 80 percent in igneous rocks.

#### 2.1.5 Water-rock interaction

The Archie's Law is only valid for conducting solutions with  $\rho_w$  equal or less than about 5 ohm-meter. For higher values of resistivity the bulk conductivity of the rock can be expressed by the formula:

$$\sigma_b = 1/F \sigma_w + \sigma_s \quad (8)$$

where

$F$  = formation factor

$\sigma_b$  = bulk conductivity of rock

$\sigma_s$  = interface conductivity

$\sigma_w$  = the water conductivity

The conductivity  $\sigma_s$  is affected by fluid-matrix interaction and depends more on the size of internal surfaces and on the formation factor than on the original chemical composition. The two main reasons for this interface conductivity are ionization of clay minerals, formed by hydrothermal alteration and surface double layer

conduction (Keller and Frischknecht, 1966).

The result of water rock interaction is that the resistivity of saturated rock can not exceed some fairly low value determined by the interaction effect.

## 2.2 The basic theory of DC-resistivity measurements

In a DC resistivity sounding a current is put into the ground and the potential difference between two points is measured at the surface of the earth. In a homogenous medium, the potential  $V$  due to a point source at the surface is directly proportional to the current  $I$  and to the resistivity  $\rho$  of the medium and inversely proportional to the distance  $r$ . The constant of proportionality is equal to  $1/2\pi$  which gives the following relation for the potential:

$$V = \frac{I \rho}{2\pi r} \quad (9)$$

If the current is injected by two electrodes,  $+I$  at  $r_1$  (source) and  $-I$  at  $r_2$  (sink) then the formula becomes:

$$V(r) = \frac{I\rho}{2\pi} \left( \frac{1}{r_1} - \frac{1}{r_2} \right) \quad \text{or,}$$

$$\rho = \frac{V(r) \cdot 2\pi}{I} \cdot \frac{1}{\frac{1}{r_1} - \frac{1}{r_2}} \quad (10)$$

Actually the earth is not homogeneous and an apparent resistivity ( $\rho_a$ ) is determined as the calculated resistivity from ( $V, I, r_1, r_2$ ) assuming the earth to be homogeneous. Using the formula it is possible to measure the resistivity for a homogeneous ground and the apparent resistivity for an inhomogeneous ground.

Several combinations of the position of current electrodes and the potential electrodes are possible when making a

DC-resistivity sounding. The most important ones are described in the following sections.

### 2.2.1 The Schlumberger Array

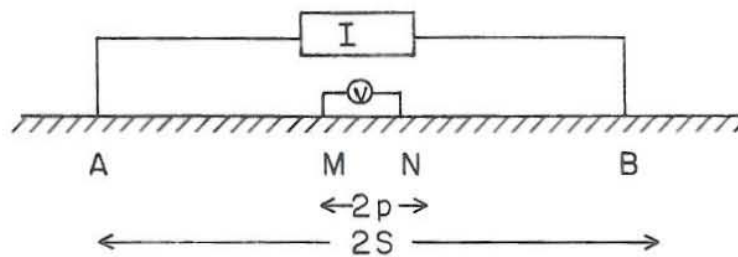


Fig 3. The Schlumberger array configuration

In this configuration the electrodes AMNB are colinear. Current injected through the electrodes A and B will create a potential which at M is

$$V_m = \frac{I\rho_a}{2\pi} \left( \frac{1}{AM} - \frac{1}{BM} \right) \quad (11)$$

and at point N it is

$$V_n = \frac{I\rho_a}{2\pi} \left( \frac{1}{AN} - \frac{1}{BN} \right) \quad (12)$$

The potential difference is  $(V_m - V_n) = \Delta V = \frac{I \cdot \rho_a}{K}$

The geometric factor K of this array of electrodes is defined as:

$$K = \frac{2\pi}{\left(\frac{1}{s-p} - \frac{1}{s+p}\right) - \left(\frac{1}{s+p} - \frac{1}{s-p}\right)} \quad (13)$$

or

$$K = \frac{\pi}{2} \cdot \frac{s^2 - p^2}{p} \quad \text{where} \quad \begin{array}{l} s = AB/2 \\ p = MN/2 \end{array} \quad (14)$$

The apparent resistivity measured in this array can also be written as:

$$\rho_a = \frac{\Delta V \cdot \pi \cdot s^2}{2 I \cdot p} \quad (15)$$

With the assumption that  $5p < s$ , we can put  $s^2 - p^2$  equal to  $s^2$  with an error less than 4% (Bhattacharya and Patra, 1968).

### 2.2.2 The head-on array

The head-on array is also called half Schlumberger array as the arrangement is similar to the Schlumberger array, except that there is one additional current electrode (c) located at infinity, i.e. at a large distance compared to AB (Cheng, 1980). The potential field at M and N is assumed to be caused by a single point electrode when the current is injected through AC or BC. This is possible because the current electrode C is located so far away from A or B.

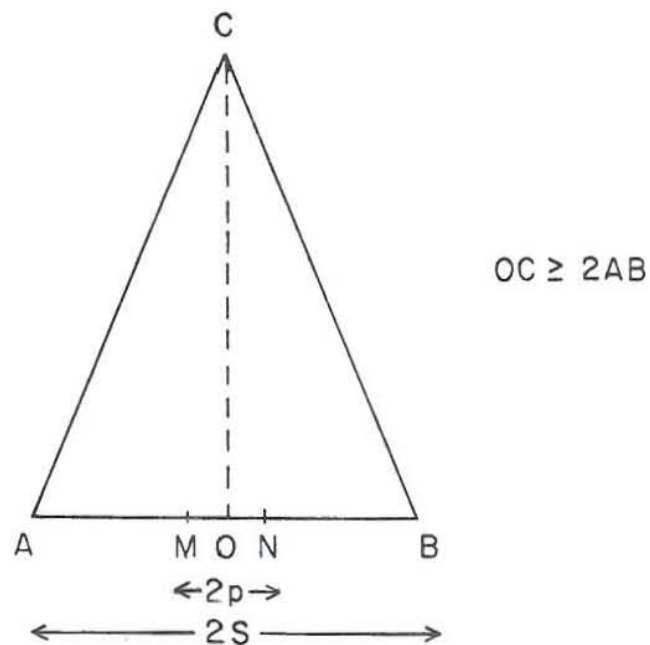


Fig 4. The Head-on array

In this case we can calculate the potential difference  $dV$  by:

$$V_m - V_n = \frac{I \cdot \rho_a^{AC}}{2\pi} \left( \frac{1}{AM} - \frac{1}{CM} - \frac{1}{AN} + \frac{1}{CN} \right)$$

with  $CN, CM \gg AM, AN$  this gives

$$\begin{aligned} V_m - V_n &\approx \frac{I \cdot \rho_a^{AC}}{2\pi} \left( \frac{1}{AM} - \frac{1}{AN} \right) \\ &= \frac{I \cdot \rho_a^{AC}}{2\pi} \left( \frac{AN - AM}{AM \cdot AN} \right) \end{aligned} \quad (16)$$

which gives us

$$\rho_a^{AC} = \frac{2\pi \cdot \Delta V}{I} \cdot \frac{AM \cdot AN}{(AN - AM)} \quad (17)$$

In the same way we get

$$\rho_a^{BC} = \frac{2\pi \cdot \Delta V}{I} \cdot \frac{BM \cdot BN}{BN - BM} \quad (18)$$

This method is used with a fixed electrode distance while the centre is moved for a certain interval (profiling). It is usually used to identify vertical structures like faults or dikes (Cheng, 1980; Flovenz and Georgsson, 1982).

### 2.2.3 The dipole-dipole arrangement

The general arrangement of the four electrodes in the dipole-dipole arrangement can be seen in Figure 5, where  $AB$  = current electrodes and  $MN$  = potential electrodes.



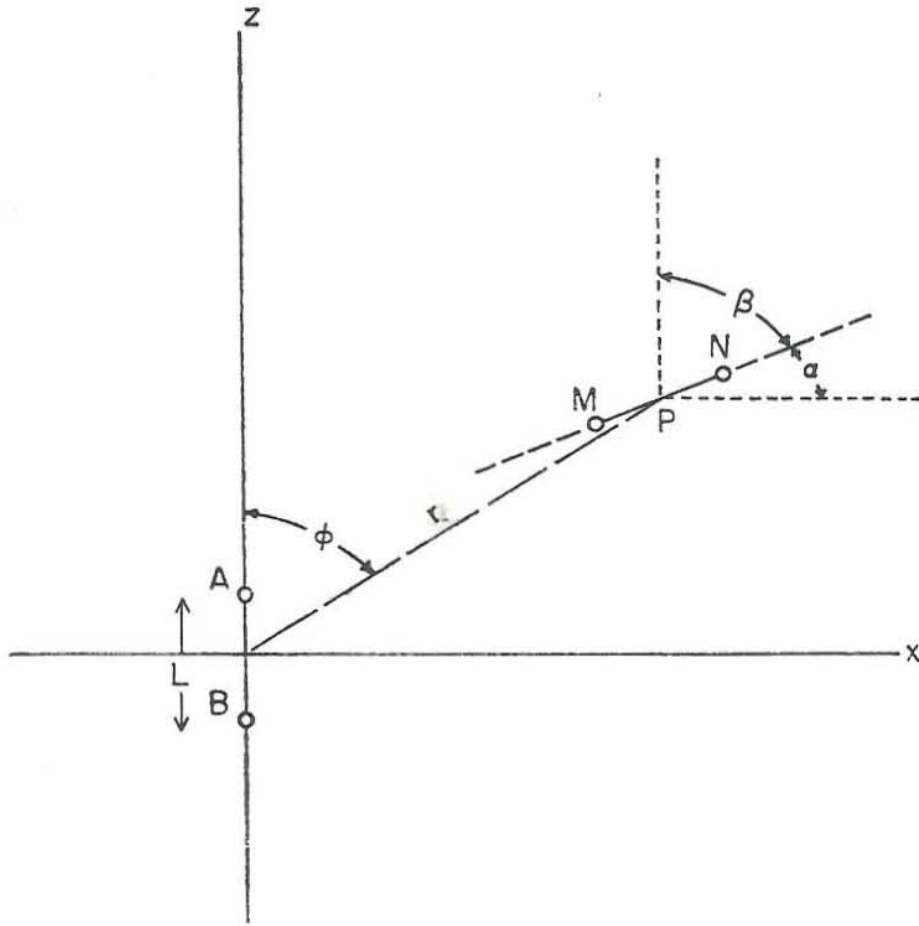


Fig 5. The Dipole-dipole array

The potential at  $r$   $V(r)$ , is equal

$$V(r) = \frac{I\rho_a}{2\pi} \left( \frac{1}{AP} - \frac{1}{BP} \right)$$

For  $r$  much larger than  $L$ ;  $V(r)_a \approx \frac{I\rho_a \cdot L \cdot \cos\phi}{2\pi r^2}$

If  $r > 3L$  the approximation error is less than 3%. From the general dipole-dipole arrangement several special arrangements have been developed.

### 2.2.4 The dipole equatorial arrangement

In this method,  $\phi$  is  $90^\circ$  and  $\alpha = 0$ : The apparent resistivity is calculated from the equation:

$$\rho_a = \frac{2\pi r^2}{L \cdot l} \cdot \frac{\Delta V}{I} \quad (19)$$

This arrangement is often used as an extension of a Schlumberger sounding because the same master curve can be used for interpretation.

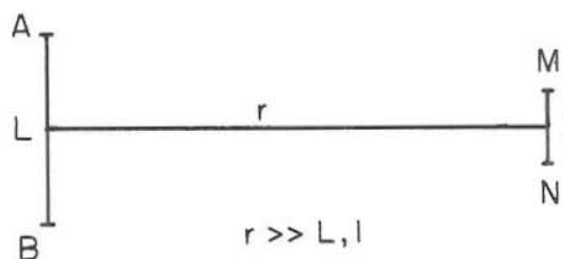


Fig 6. The dipole equatorial array

### 2.2.5 The dipole-axial arrangement

In this arrangement the angle of  $\phi$  and  $\alpha$  are equal zero and the apparent resistivity is obtained from:

$$\rho_a = \frac{\pi \cdot R^3}{L \cdot l} \cdot \frac{\Delta V}{I} \quad (20)$$

This array is often used as a profiling method.

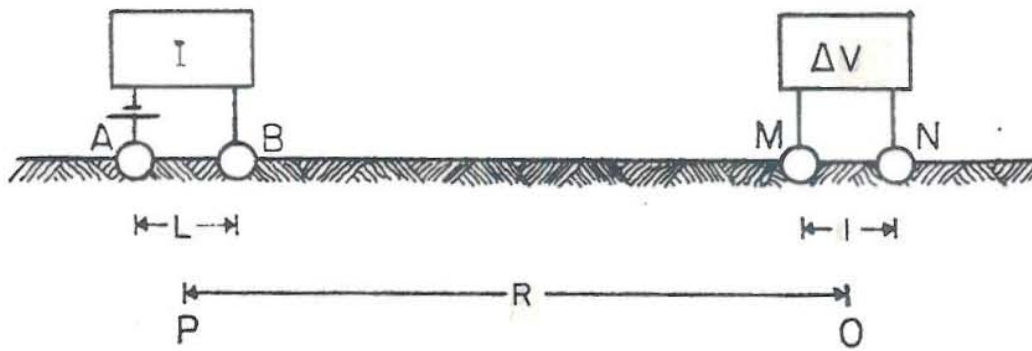


Fig 7. The dipole-axial arrangement

### 2.3 Field techniques

The profiling techniques are often used in a reconnaissance survey. A fixed electrode spacing is chosen and the central point moved along a straight line, e.g. a road or a track. The interval between measurement stations is usually fixed, for example  $AB/2$  at 250 m and 500 m if the Schlumberger set up is used.

In head-on profiling a suitable fixed electrode spacing is used and selected on basis of the results of the Schlumberger sounding data in the same area. The azimuth of the line should if possible be perpendicular to the strike of the structures in the area if possible. The interval of the measurement stations is usually very dense, usually about 25 m as for example in a survey in which the author participated in the Selfoss area, Iceland. The electrode at infinity (C) is located about 5-10 km from the central point O of the profile with OC usually semi-perpendicular to the direction of the AB-line. Several measurements are done to get a reliable value at each of the parameters  $\rho^{AB}$ ,  $\rho^{AC}$  and  $\rho^{BC}$ .

In geoelectric depth soundings with the Schlumberger method, the measurements are made by starting with the smallest spacing of AB and then increasing it in logarithmic steps. For each spacing  $\rho_a$  values are calculated. The spacing of  $AB/2$  is usually varied from 1-10 m up to 1-2 km,

depending on the sensitivity of the instruments and the target.

The corresponding potential electrode spacings,  $MN/2$ , are typically varied from about 0.2-1 m up to 80 m, increasing with increasing  $AB/2$ . The depth penetration of the current increases with increasing separation of the electrodes. The results of the resistivity measurements are plotted on a double-logarithmic paper.

In dipole-dipole soundings the dipole lengths ( $L$  and  $l$ ) are usually of the order of 100 to 1000 m and the distance  $r$  has a range of up to 7 to 10 km. A powerful equipment is needed to get a good depth penetration (several amperes at least).

#### 2.4 Instrumentation

The equipment needed to conduct the measurements consists of a transmitter unit and a receiver unit.

The transmitter usually operates at about 1000 volts maximum and creates a maximum current of 0.1 ampere for small equipment but up to 30 amperes in large instruments. The transmitter sends a square wave current, with regulated pulse lengths of e.g. 2, 4 or 8 seconds. The currents are transmitted through wires and injected into the ground through two electrodes. The current-electrodes are usually made of iron, aluminium or copper spikes to ensure a low contact resistance with the ground.

The receiver console consists of a highly sensitive voltmeter with a biasing circuit and filtering device to remove electrical noise. The potential electrodes should have a low electrical noise generation at the contact with the ground. The most common ones are  $CuSO_4$  porous pots (nonpolarizing type).

The transmitter and voltmeter may be coupled together so the measurement can be performed automatically as well as in a manual way. A processor, used to stack the reading and calculate the average and the standard deviation of the measurement, may also be incorporated in the instruments. This is the case of the equipment designed in Iceland and used at Orkustofnun, the National Energy Authority (NEA).

### 2.5 Measurement errors

In order to obtain good quality data in geoelectric measurements measurement errors should be avoided at all cost.

Among common causes for and simple remedies are:

- a) Current leakage in wires and reels should be checked. This leakage can be the source of too high voltage readings. The current and receiver circuits should be kept well separated and wet conditions should be avoided.
- b) Wire fences, buried pipelines and telephone cables should be avoided as these can distort the signal and will thus create false apparent resistivity curves.
- c) The influence of the skin effect can affect the results if the transmitter is operated at too high a frequency.
- d) By neglecting the contact resistance correction the apparent resistivity measurement may become too small.

### 2.6 One-dimensional Schlumberger interpretation

To interpret the Schlumberger sounding data the values of  $\rho_a$  against  $AB/2$  are plotted on a log-log paper. The interpretation of these curves leads to a model of the

earth consisting of several layers, each having a true resistivity and thickness. There are several ways to carry out the interpretation. We divide them into complete and partial curve matching and forward and inverse computer modelling.

In complete curve matching an album of master curves for two, three or four layers are used. By finding a master curve similar in shape to the field sounding curves a layered model is found. From a master curve showing a good fit the information of the ratio of resistivities of the layers and the ratio of the thicknesses can be read.

In the partial curve matching, sometimes called the auxiliary point method, two layers are combined into one equivalent layer with the help of auxiliary diagrams and then 2 or 3-layer master curves used for matching. The details of this technique are described by Keller and Frisnecht (1966), Orellana and Mooney (1966) and by Bhattacharya and Patra (1968).

The one dimensional interpretation can also be done with the aid of a computer e.g. with a program called VIDNAM at NEA in Iceland. As an input data a guessed model is inserted and then the computer calculates the apparent resistivity curve for the given model. If the calculated resistivity curve does not fit to the apparent resistivity curve (this can for convenience be displayed on a terminal screen), a new modified model is inserted into the computer. This visual trial and error method is then continued until a good fit has been achieved (Johansen, 1975).

The inverse modelling is an automatic interpretation technique done by the computer (e.g. a program called CIRCLE at NEA). A guessed model is inserted as an input data, then the iterations are done automatically by the computer until a good fit is found (Johansen, 1977).

### 2.7 Two dimensional interpretation

In the interpretation of HEAD-ON profiling data, the main object is to map near vertical faults or dykes. This is a 2-dimensional interpretation. If the AB array crosses a steeply dipping conductive fault, the changes of  $\rho_a AC$  and  $\rho_a BC$  across a steeply dipping fault can be expected to be somewhat similar to the one in Fig 8, where the cross over defines the location of the fault. The dipping of the fault can sometimes be assessed by using different AB/2 spacing and by that getting a cross over corresponding to different depth of penetration. A computer interpretation is possible with the use of a 2-dimensional program (Dey and Morrison, 1976).

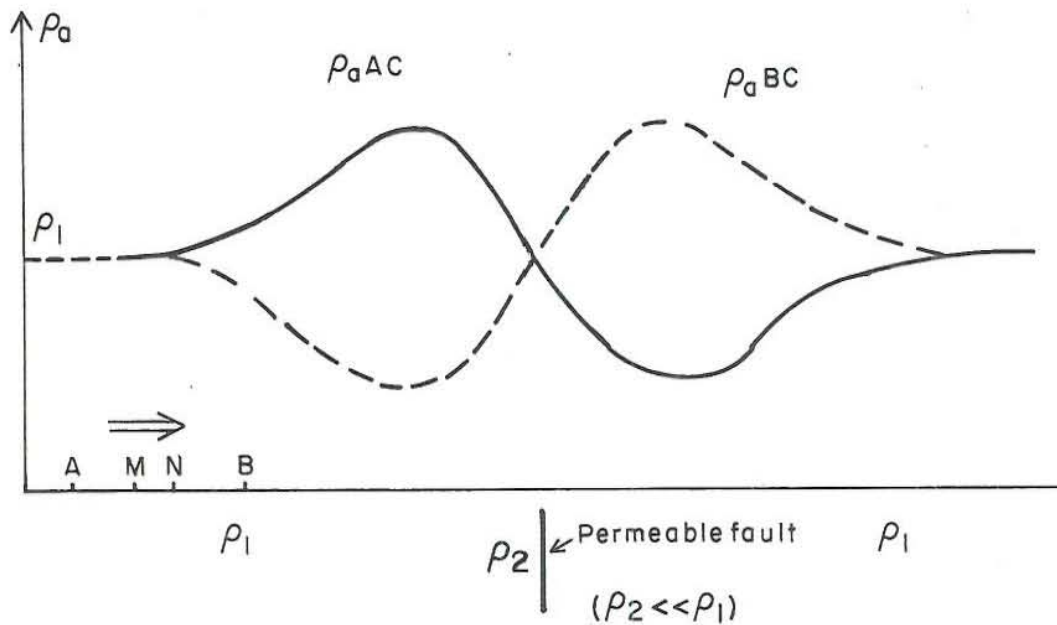


Fig 8. Changes of  $\rho_a AC$  and  $\rho_a BC$  across a fault.

A model of resistivity structures is inserted in the computer and by successive visual iteration as good a fit as possible with the field curve is obtained.

### 3. GEOTHERMAL ACTIVITY IN THE CISOLOK-CISUKARAME AREA

#### 3.1 Introduction

The Schlumberger sounding resistivity measurements of the Cisolok and Cisukarame areas have been made in two periods. In 1976 the West Japan Engineering consultants measured 73 stations with 500 m spacing along 10 traverse lines distributed in the Cisukarame, Cisolok and Sangiang areas. In 1982 the author lead an exploration team of the Geothermal Division of Pertamina which measured 80 additional stations along 10 traverse lines (Alhamid and Hantono, 1982). From the total of 150 measured stations only 69 were selected for the detailed analysis and interpretation presented in this report. The other 83 were of rather low quality and not suitable for computer modelling. The location of the soundings and cross sections are shown on a map in a pocket of the back of the report.

In the Cisukarame are 5 lines were selected. Each line usually has 8 soundings except the D-line, which has 10 soundings and the E-line with 5 soundings. The spacing between the soundings is usually 500 m except in the D-line, where it is sometimes 200-300 m. Two lines were selected from the Cisolok area. Each line contains 7 soundings spaced 500 m apart. All these soundings have a maximum current arm ( $AB/2$ ) of 1000-2000 m, with the lower values belonging to soundings at the ends of the lines. All the data were interpreted by the program CIRCLE (automatic 1-dimensional interpretation) and plotted by a plotter using the program VIDPHI in the computer at NEA. The data, the 1-dimensional interpretations and the corresponding calculated curves are shown in Appendix I. The results of the resistivity measurements will be discussed in this report and a resistivity model presented for the geothermal field.

The aim of the measurements was to delineate the geothermal



area and to site several shallow wells to measure the thermal gradient in the area. A site for a deep well is also proposed using the resistivity results.

Several other investigation methods were applied in the area and reported on by the West Japan Engineering Consultants (1976), such as geological mapping, analysis of rock alteration, and chemical analysis of water samples collected from several hot springs in the Cisolok and Cisukarame area. Pertamina has also drilled about 15 shallow thermal gradient wells in the area.

### 3.2 Geological setting

The Cisolok-Cisukarame geothermal area is located near the town of Pelabuhan Ratu near the south coast of West Java. It is within the southeastern part of the Bayah Mountain which constitutes a large dome, called the "Bayah Dome" and several upper Pleistocene volcanoes (Figure 9). The lithology of the Bayah Mountain has been divided into 10 lithological units which range in age from Eocene through Pleistocene (Bemmelen, 1949).

In his schematic diagram for the lithological column of the Bayah Mountain, van Bemmelen (1949) indicates that the Upper Pleistocene volcanoes of Malang, Endut and Halimun are underlain by an approximately 500 m thick sequence of andesite lavas, breccias and tuffs of Plio-Pleistocene age which in turn is underlain by a more than 1000 m sequence of mostly shallow water sediments with minor intercalations of lavas of Eocene to Miocene age. The sedimentary sequence is intruded by granodiorite intrusions and rhyodacite domes of Miocene age. The sediments consists of numerous layers of conglomerate, sandstone, mudstone, tuff, lignite, marl and limestone.

The lithology of the Cisolok-Cisukarame area can be divided into 3 major groups, a) the sedimentary rocks of Lower

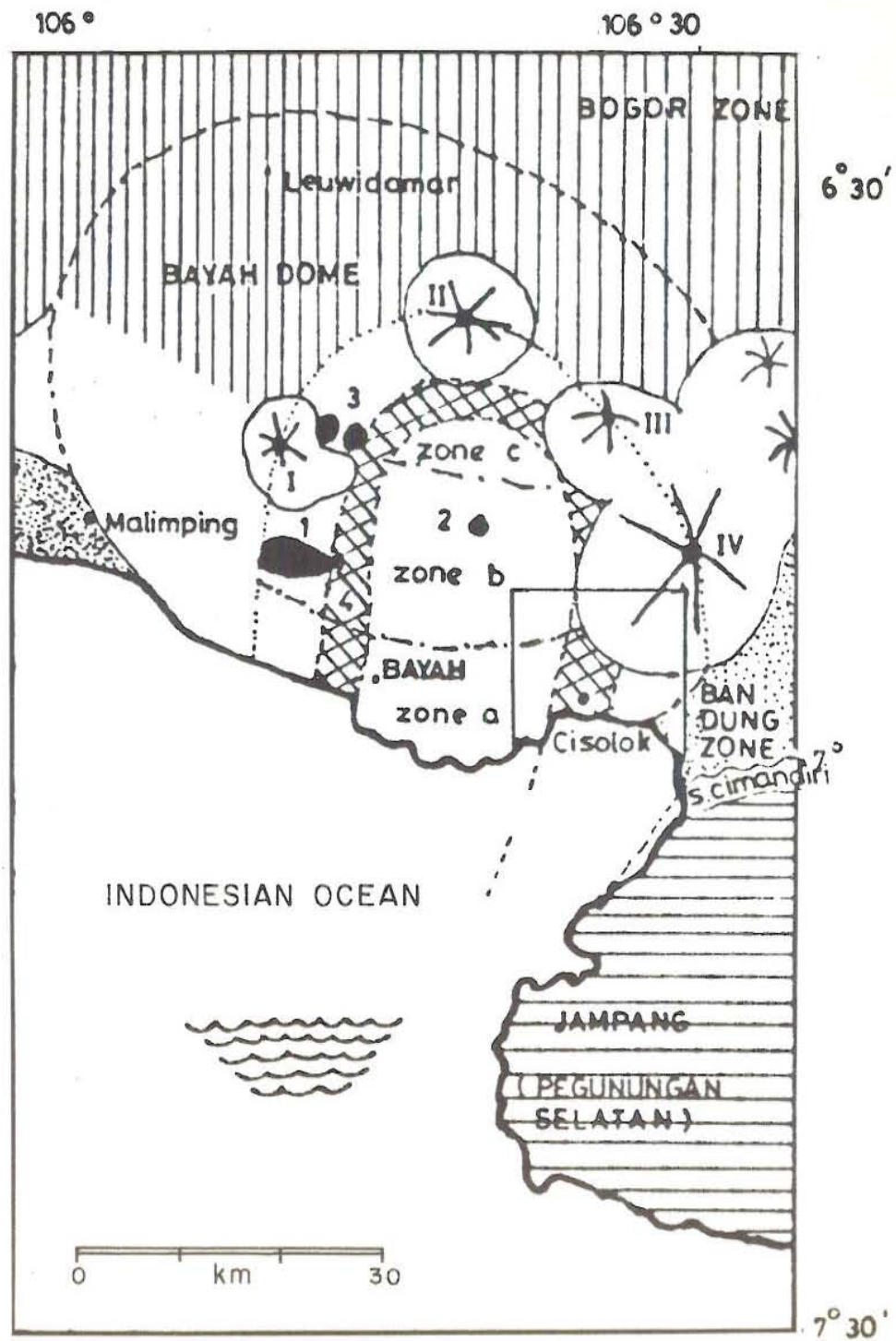


Fig. 9. Physiographic schetsmap of the Bayah Dome Pelabuhan Ratu, West Java, Indonesia.

Miocene through Lower Pleiocene, b) andesitic and dacitic intrusions of Miocene age and c) andesitic lavas of Pleistocene age.

### 3.3. Geothermal surface manifestations

Geothermal surface manifestations occur at three localities in the Cisolok-Cisukarame region.

#### 3.3.1 The Cisukarame area

The Cisukarame area has the most powerful surface manifestation of the three geothermal areas in the Cisolok-Cisukarame region. There are many hot springs distributed along the Cisukarame river, one of which discharges boiling or nearly boiling water of a very large amount. The West Japan Engineering Consultants (1976) estimated the flow from the spring to be about 217 l/s, and they reported altered rocks to be scattered in an area of about 4.5 km<sup>2</sup>. In addition, a strongly altered zone of 800 m x 500 m in size is found approximately 1.5 km north of the Cisukarame hot springs. In this area there are two fault systems; one with a NW-SE trend and the other with a N-S trend. The thermal manifestations are mainly distributed along the NW-SE faults. The hot spring waters are saline and are considered to be formed by a simple dilution of high temperature deep water with surface water; the maximum underground temperature calculated from the chemical constituents of the hot springs is reported 193°C by the West Japan Engineering Consultants (1976).

The underground temperatures were calculated in Iceland from the same analysis using the Na/K and silica geothermometers. The results indicated temperatures in the range of 150-175°C and showed that the quartz temperature and the Na/K temperature compare quite well for waters in the area (Einar Gunnlaugsson, pers. comm., 1982).

### 3.3.2 The Cisolok area

In the Cisolok area, geothermal manifestations such as fumaroles, hot springs and altered ground are mainly distributed in a 25 km<sup>2</sup> area along the NNE-SSW trending main faults and the NW-SE trending subfaults that cut the Cisolok acidic complex. The faults probably provide a passage for the thermal fluids. Boiling or near boiling springs are found at some twenty localities along the Cipanas river. The results of chemical analysis of hot waters and gases indicates that shallow ground water is heated by steam rising from greater depths; the maximum underground temperatures computed from the chemical constituents of the waters are only reported 113°C by the West Japan Engineering Consultants, (1976).

Calculations in Iceland of the Na/K and silica geothermometers using the same analysis indicate on the other hand that the underground temperature in the Cisolok area is probably in the range of 125-160 °C (Einar Gunnlaugsson, pers. comm., 1982).

### 3.3.3 The Sangiang area

In the Sangiang area strongly altered and silicified rocks are found in an area of about 2 km<sup>2</sup>, but no hot springs are found. The existence of mixed-layer clay minerals indicates temperatures of the rocks having been well above 100 °C (West Japan Engineering Consultants, 1976).

### 3.4 The data quality and interpretation

In general it must be said that the Schlumberger soundings data in the Cicukarame and Cisolok areas are not of a high quality. The data are scattered and some of the new soundings rise too steeply ( $>45^\circ$ ) near the end.

It must however, be stressed that the topography and the geology are very complicated in the area so it is not an easy task to measure good quality soundings there. This is probably the main reason for the scattered data. There are several factors that can cause the too steeply rising soundings. For example, it is possible that induction influences the measurements, so the results become too high. The reading period may be too short, or possibly for the longer AB/2 spacings the self potential noise of the instruments and electrodes may not have been properly eliminated.

All the data were analysed and interpreted 1-dimensionally and one cross-section in Cisukarame was interpreted 2-dimensionally.

In the Cisolok area the soundings were located nearby parallel with the contact of a conductive body (saline sediments) and a body with a higher resistivity. This affected the soundings very much and made 1-dimensional interpretation difficult. This could not be corrected with 2-dimensional interpretation as the 2-dimensional program assumes soundings crossing structures at right angles ( $90^\circ$ ) but not being parallel to them.

Because of this, the accuracy of the 1-dimensional interpretation of the Cisolok data is open for question and this was also the reason why only a rough estimate of some soundings was used.

It must, however, be remembered that difficult topography

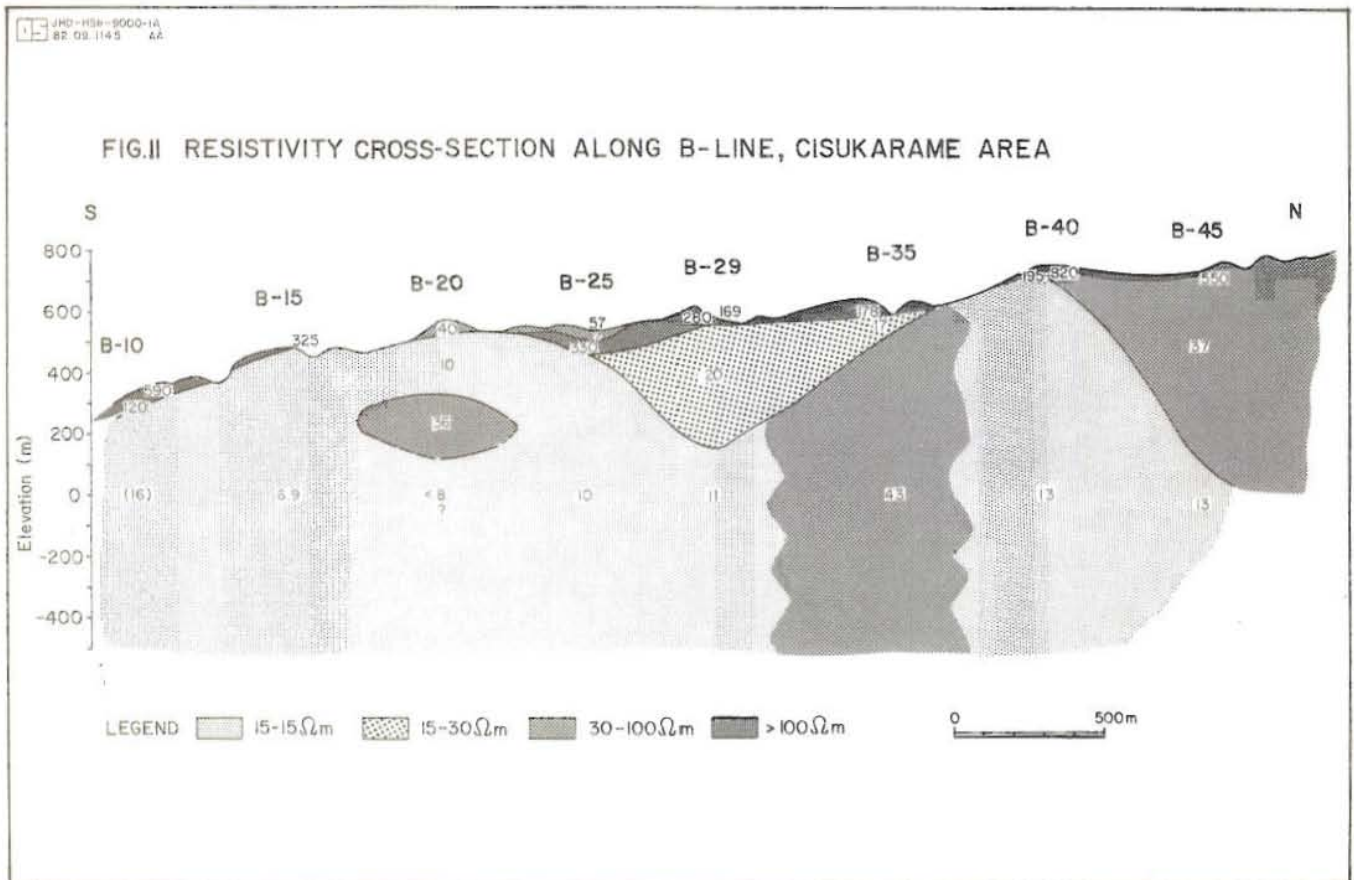
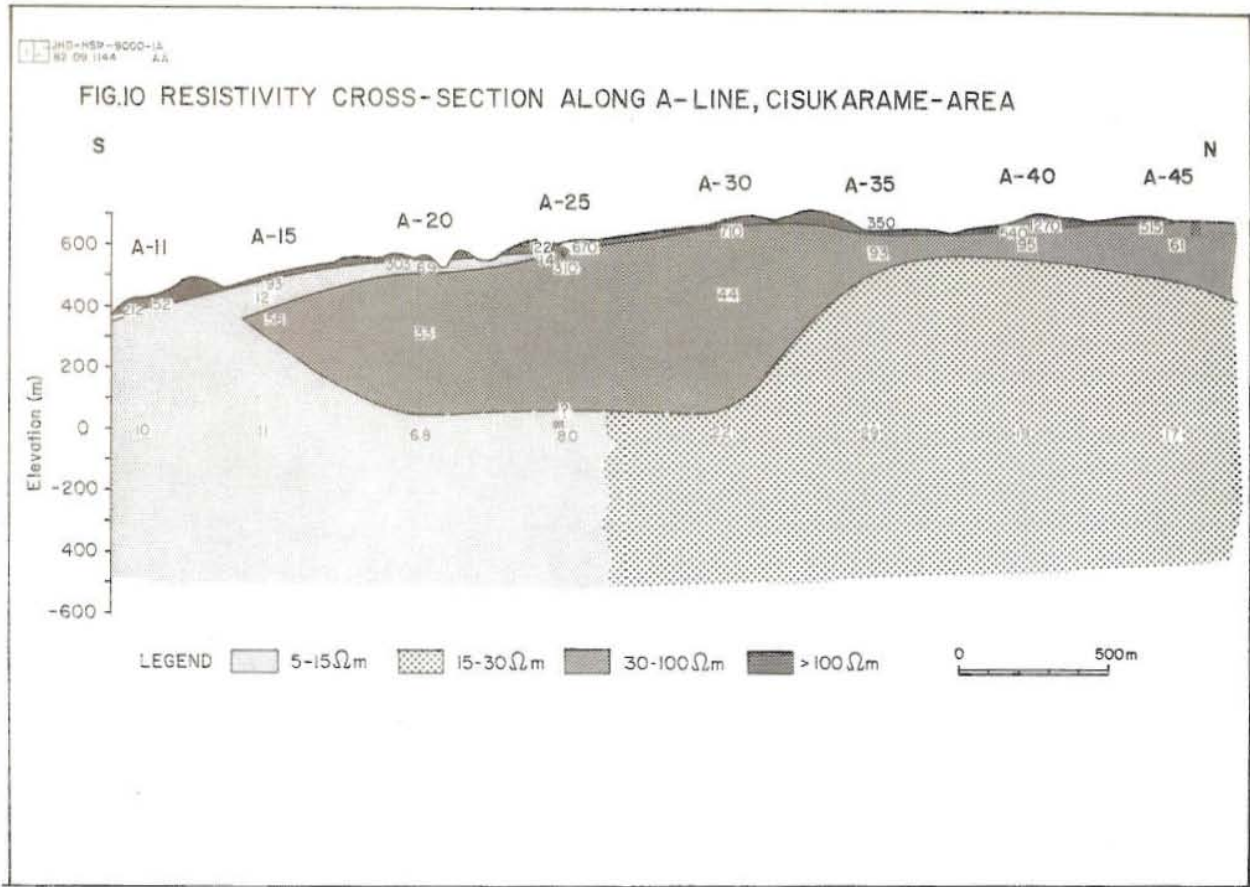
can make it infeasible to measure the soundings in lines at right angles to the structural trends. Another resistivity technique must probably be used if good results are to be obtained in Cisolok.

### 3.5 Cisukarame 1-dimensional interpretation

Five cross-sections were made of the resistivity structure of the area and will be discussed below.

Cross-section A: This cross-section (Fig. 10) includes 8 soundings and runs with a NW-SE direction along the western part of the Cisukarame area. The first layer is thin and has a resistivity of more than 100 ohmm. It can be correlated to a pyroxene andesite lava which covers most of the surface in the area. The second layer has a resistivity of 30-100 ohmm; it is 300-500 m thick and can be correlated to a tuff breccia and andesite. A third layer with a relatively low resistivity (5-15 ohmm) is found in the southern part of the section. This low resistivity zone has a width of about 1.5 km and can be correlated to a sedimentary formation (the Cimaja formation) which consists of sandstone, mudstone and a basal conglomerate. The connection between this formation and the geothermal field will be discussed in conjunction with the iso-resistivity map. To the north this layer is terminated by a medium resistivity layer of 15-30 ohmm.

Cross-section B: The resistivity layering (Fig. 11) is similar to cross-section A. The near surface resistivity is more than 100 ohmm which can be correlated to the pyroxene andesite. The medium resistivity layer of 15-30 ohmm can be found below soundings B-25 to B-35 with a thickness varying symmetrically from nil at both ends to about 300 m below B-29. The third layer of 5-15 ohmm can be seen almost in the whole cross-section. This layer can be correlated to the same sedimentary formation (the Cimaja formation) as in cross-section A. The layer is apparently



intruded by a relatively high resistivity body (43 ohmm) below sounding B-35.

Cross-section C: As in sections A and B the uppermost layer (>100 ohmm) in this section (Fig. 12) can be correlated to the pyroxene andesite. The second layer has a resistivity of 5-15 ohmm and can be correlated to the sedimentary (Cimaja) formation. The third layer has a very low resistivity, less than 5 ohmm and may represent either a high salinity water bearing formation or an intensely altered zone. High salinity is a more likely explanation, especially if one compares it with the 200-300 meter thick layer of 3-5 ohmm in Cisolok.

Cross-section D: The high resistivity surface layer corresponding to the pyroxene andesite is only detected from D-30 to the northern part (Fig. 13). This layer is underlain by two distinct layers with resistivities of 30-100 ohmm and 15-30 ohmm successively. The lowest resistivity layer less than 5 ohmm can be found southwards from D-27, and is believed to represent high salinity. Below this conductive layer a relative low resistivity layer of 5-15 ohmm is found. The lowest values for this layer are measured nearest to the hot springs and probably reflect the geothermal influence, even though the resistivity of the formations is low.

Cross-section E: As seen in Fig. 14 the high resistivity layer (>100 ohmm) representing the pyroxene andesite can be found in the whole cross section except below sounding E-30 in the south. It is underlain by a layer with a resistivity of 15-30 ohmm in the middle and southern part of the area. In the middle of the area a third resistivity layer of 5-17 ohmm occurs which can be correlated to the sedimentary (Cimaja) formation. A medium and high resistivity bodies in the southern and northern parts of the section show a diffuse boundary with the conductive zone in the middle of the section.



FIG.12 RESISTIVITY CROSS-SECTION ALONG C-LINE, CISUKARAME-AREA

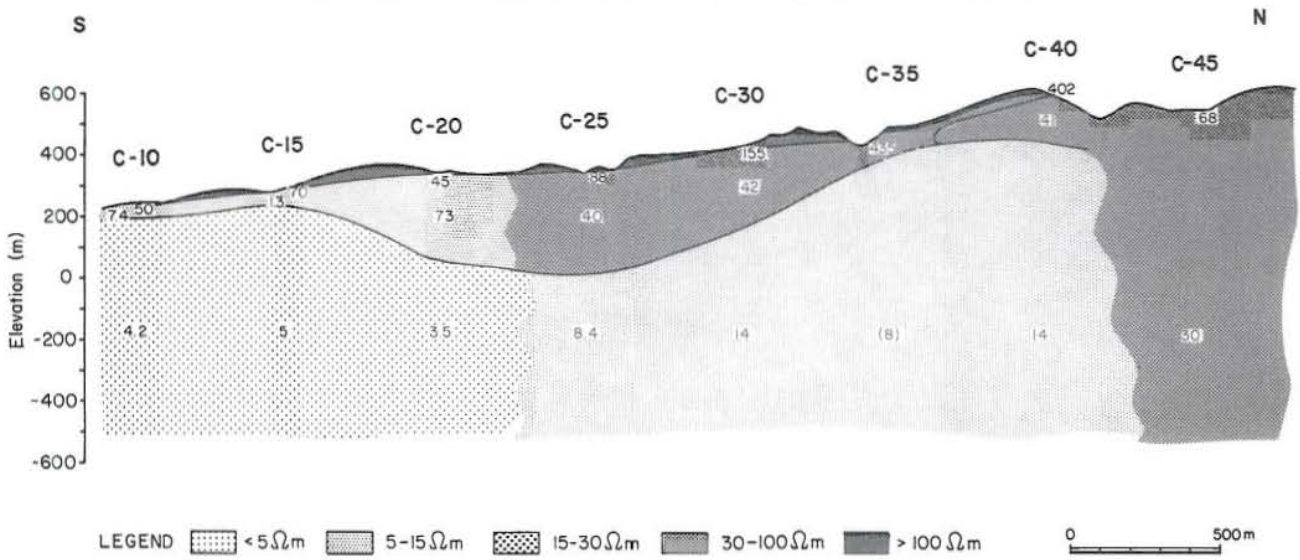


FIG.13 RESISTIVITY CROSS-SECTION ALONG D-LINE, CISUKARAME

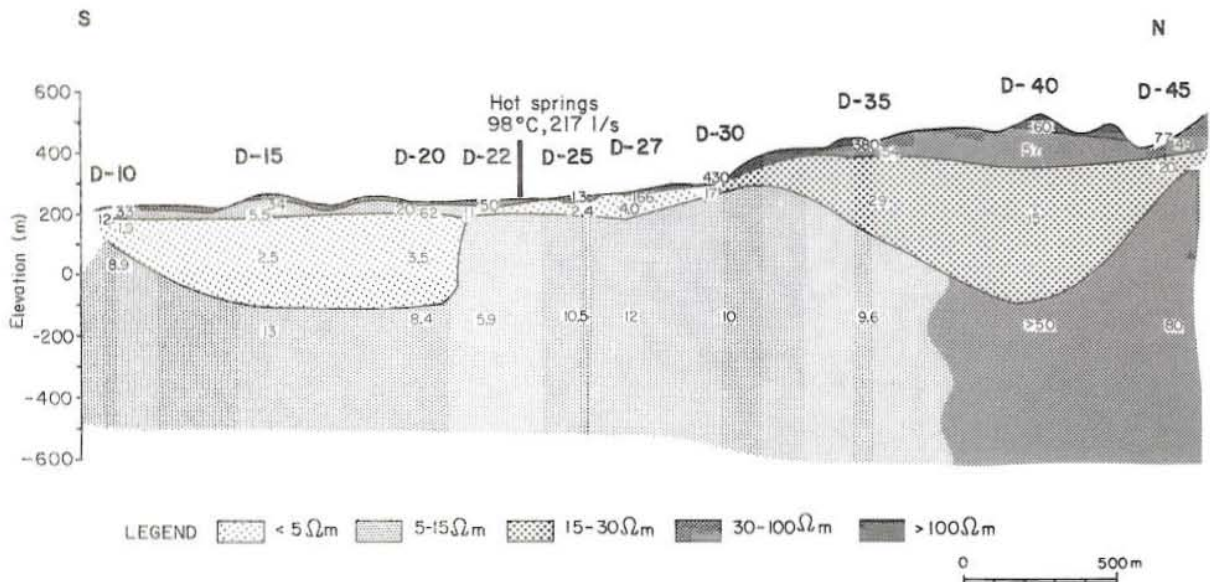
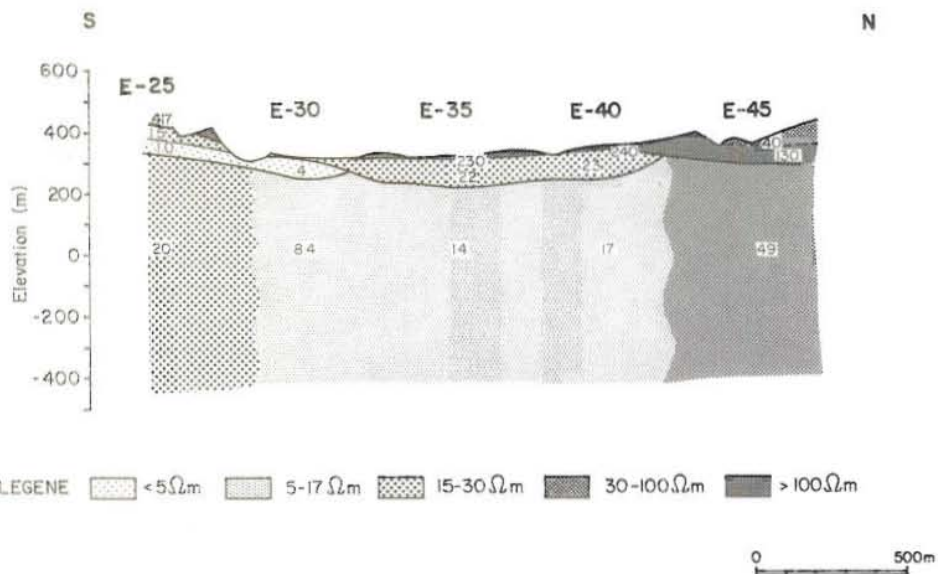


FIG.14 RESISTIVITY CROSS-SECTION ALONG E-LINE, CISUKARAME-AREA



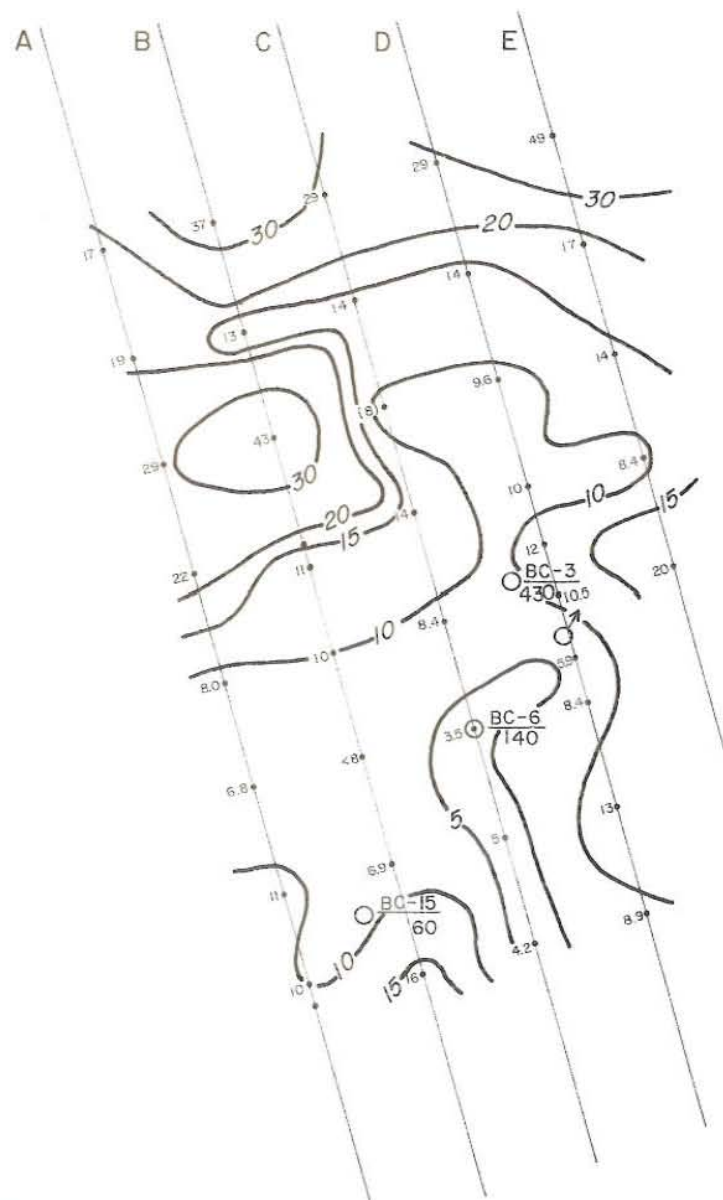
### 3.5.1 The Cisukarame Area Isoresistivity Map

The Iso-resistivity map of Cisukarame (Fig. 15) shows an isoresistivity map of the Cisukarame area at a depth of approximately 500 m below the surface. The map can be divided into two parts. In the northern part the resistivity is generally rather high, 15-40 ohmm. In the southern part the resistivity is generally low, less than 15 ohmm. The map shows a low resistivity anomaly (<10 ohmm) in the center of the area of investigation but open towards south (as the soundings were measured). The lowest resistivity values are recorded in the soundings C-10 - C-20 or some 3-5 ohmm. This low resistivity layer has been correlated to the Cimaja formation which consists of marine sediments, clay and tuffs. The formation seems to have a low resistivity in general due to salinity and the clay content. But the hot springs are also found within this area. The question then arises in what way can this low resistivity anomaly be attributed to the upflow of the geothermal fluid. This question is very difficult to answer but some guidelines can be given. In general we can not assume that the low resistivity anomaly is caused by the geothermal fluid. The heat-gradient in the shallow drillholes confirms this. One possibility is that the upflow zone of the geothermal fluid is 0.5-1.0 km north of the hot springs indicated by the low resistivity values measured in the center of the area of investigation. It must then be assumed that the geothermal fluid flows laterally towards south before reaching the surface at low elevation in the valley carved by the Cisukarame river. An extensive zone of strongly altered rocks in this area could be a confirmation of this theory. The same applies for the high heatflow (430°C/km) measured in a drillhole BC-3, 300 m north of the hot springs. This also strengthens the theory.

Fig. 15

**ISORESISTIVITY - MAP  
CISUKARAME - AREA**


(500m BELOW SURFACE)

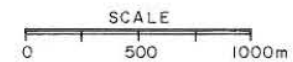


**LEGEND**

 Contour in Ohm meter

 Hot spring

  $\frac{BC-3}{430}$  Shallow hole and thermal gradient value ( $^{\circ}C/km$ )



### 3.6 Cisukarame 2-dimensional interpretation

The 10 Schlumberger soundings belonging to the D-line were interpreted 2-dimensionally. In the vicinity of the hot springs the soundings are spaced at 200-300 m intervals instead of the usual 500 m.

In the 2-dimensional interpretation we assume that all structures have an "infinite" extension towards west and east and it is very doubtful whether these conditions are fulfilled. The field resistivity pseudosection and the calculated pseudosection derived from the model calculations are shown in Fig. 16.

The starting model was based on the 1-dimensional interpretation, but by several iterations the model was modified, until a satisfactory result was reached. The calculated pseudosection derived from the model is fairly similar to the field pseudosection.

The resistivity model shows the lowest resistivity values at depth (8 ohmm) near the hot springs.

As discussed in the former chapter it is very difficult to distinguish between the low resistivity measured in the Cimaja formation and low resistivity caused by the geothermal fluid. But it was proposed there that the upflow of the geothermal fluid is 0.5-1.0 km north of the hot springs. According to the 2-dimensional interpretation the low resistivity zone stretches even further north.

### 3.7 Cisolok, 1-dimensional interpretation

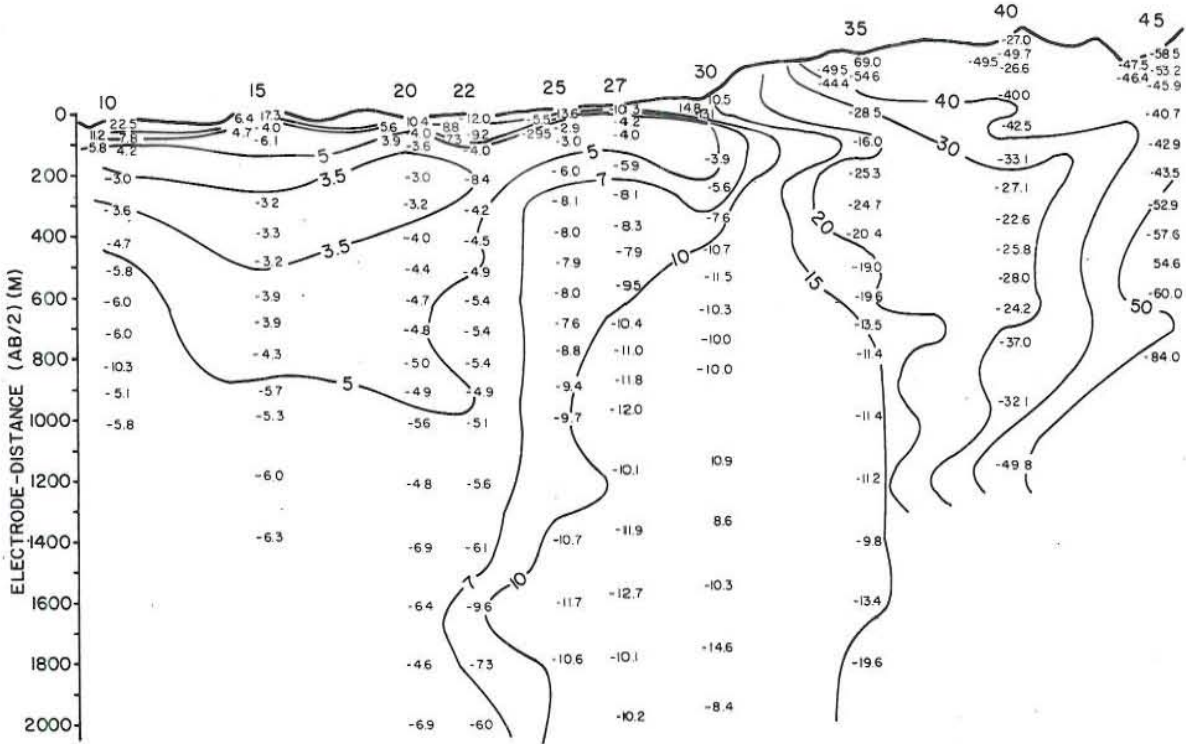
Cross-sections A and B: The uppermost layer of both cross-sections A and B (Fig. 17 and 18) has a low resistivity of 5 to 30 ohmm, corresponding to alluvium, tuff and saline sediments. The conductive zone below the surface with a resistivity of less than 5 ohmm is found all

JHD-HSB-9000-1A  
82.10 1181 AA

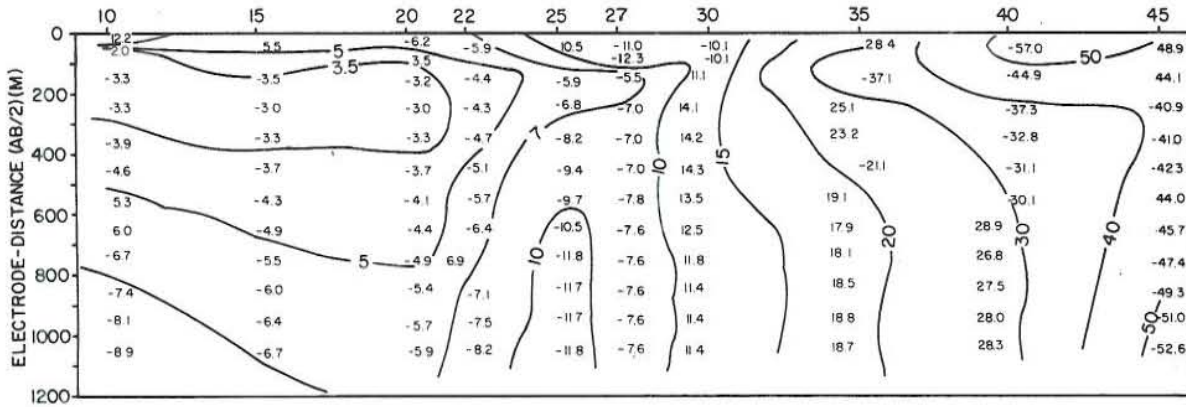
### CISUKARAME D-LINE

Fig. 16

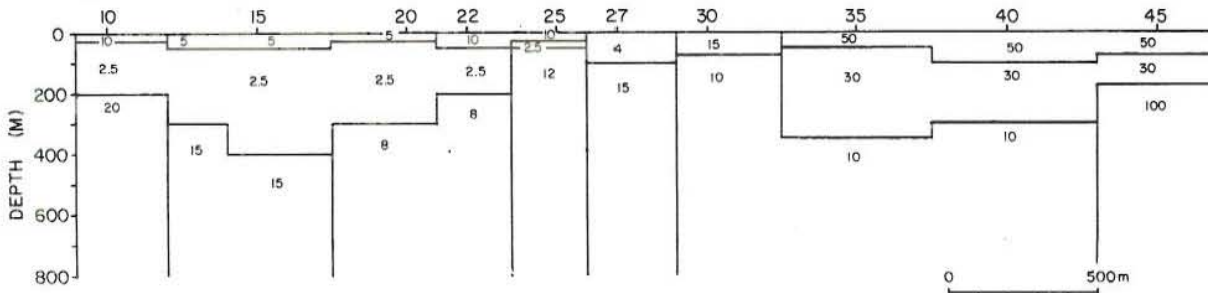
#### A. FIELD RESISTIVITY - PSEUDOSECTION

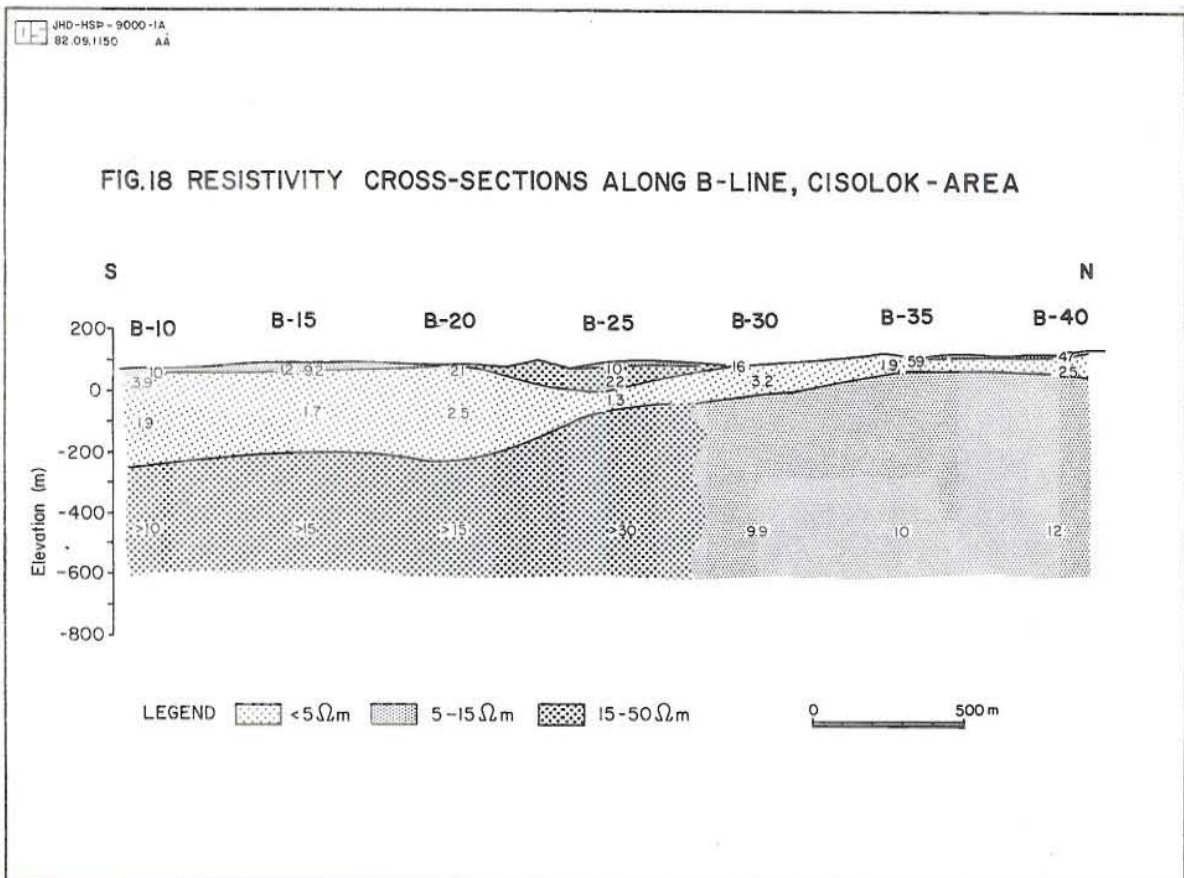
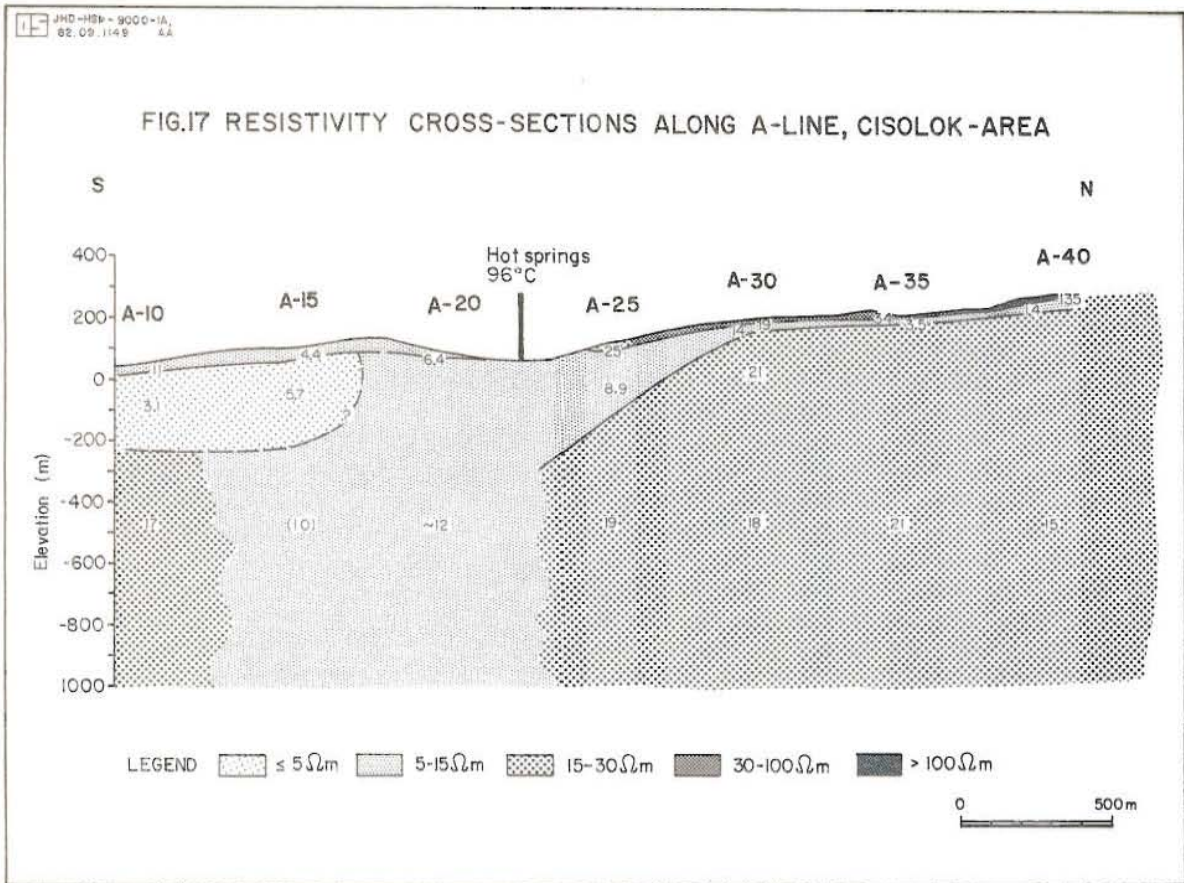


#### B. CALCULATED RESISTIVITY - PSEUDOSECTION



#### C. TWO DIMENSIONAL RESISTIVITY MODEL





along cross-section B, but only in the southern part (A10 - A15) in cross-section A. These layers can probably be correlated to sedimentary layers containing sea-water. A shallow hole (BC-12) drilled in this area 500 m south of A-10 shows a thermal gradient of 80°C/km. Only the third layer with a resistivity of 5-15 ohmm found in A-20 and A-25 may possibly be connected to the geothermal system evidenced by the existence of the hot springs. A hole drilled near A-20 (BC - 8) shows a high thermal gradient of 310°C/km indicating convecting hot water. This layer belongs to the Cimaja sedimentary formation. Similar values were found in soundings B-30 to B-40. The fourth layer noticed in the cross sections has a resistivity of 15 - 30 ohmm north of A-25, but is not found in cross-section B.

### 3.8 Conclusions

(1) The resistivity pattern at depth in the Ciskuarame area shows a low resistivity zone (<10 ohmm) in the middle of the area of investigation. This zone is open to the south. The center of the anomaly does probably reflect the center of the geothermal system, as it coincides with an area of high thermal gradient and altered rocks. The hot springs are found in the valley carved by the Cisukarame river to the south of the anomaly. This may be explained by lateral flow from the upflow zone in the highlands towards lower elevations due to hydrostatic gradient.

(2) The most conductive layer in Cisukarame and Cisolok which has a resistivity of 3-5 ohmm and a thickness of 100-300 m is thought to correspond to a sedimentary formation containing water of high salinity.

(3) Reinterpretation of chemical data from the hot springs by Einar Gunnlaugsson (Pers. comm., 1982) with the Na/K and Silica geothermometers indicates temperature in the geothermal systems to be in the range of 150-175°C in the

Cisukarame area and in the range of 125-160°C for the Cisolok area. The two geothermometers gave similar results.

(4) The results of 2-dimensional modelling in Cisukarame indicated a larger low resistivity zone (geothermal field) than suggested by the 1-dimensional interpretation. Further the 2-dimensional interpretation shows more clearly the vertical boundaries of the layers.

### 3.9 Recommendations

From a close examination of the Cisolok-Cisukarame exploration results a special emphasis has been put on the resistivity measurements. The author would like to recommend further exploration steps as follows:

a) In Cisukarame area a more detailed geological mapping on a scale of 1:10,000 is needed to define the lithological boundaries more clearly.

b) Detailed magnetic measurements are suggested to be done in a similar scale in the Cisukarame area. Preferably this should be a low altitude (100 m) aeromagnetic survey but ground magnetic survey with the dense station interval of 25 m or 10 m might also be of great value in selected localities. The aim of the measurements would be to map the alteration zones at depth, but intense alteration usually creates a negative anomaly compared to the surroundings.

c) It should be considered whether other resistivity methods for example MT, would delineate the resistivity structure of the area more clearly and thus give better information on the size of the geothermal fields.



d) To check the low resistivity area in the northern and central part of the area, where the spacing of existing shallow holes is not dense. It is advisable to drill there several additional shallow thermal gradient wells of 100-200 m depth.

e) To understand more clearly the origin structure and the heat source in this area, probably originating from intrusions, it is recommended to do a detailed gravity survey.

## ACKNOWLEDGEMENTS

First of all the author would like to express his gratitude to the management of the UNU Geothermal Training Programme 1982 held at the National Energy Authority of Iceland especially to Dr. Ingvar Birgir Fridleifsson and Dr. Axel Bjornsson. The author is much indebted to Ludvik S. Georgsson for his supervision and his patient guidance during the training course and in the preparation of this report.

Also the author would like to thank all lecturers for their valuable lectures during the introduction and practical courses.

Special thanks to Sigurjon Asbjornsson for processing and computer editing the manuscript. Thanks are also due to the drafting section of the NEA who drew all the figures in this report.

I am grateful to the UN University for the award of the UNU Fellowship.

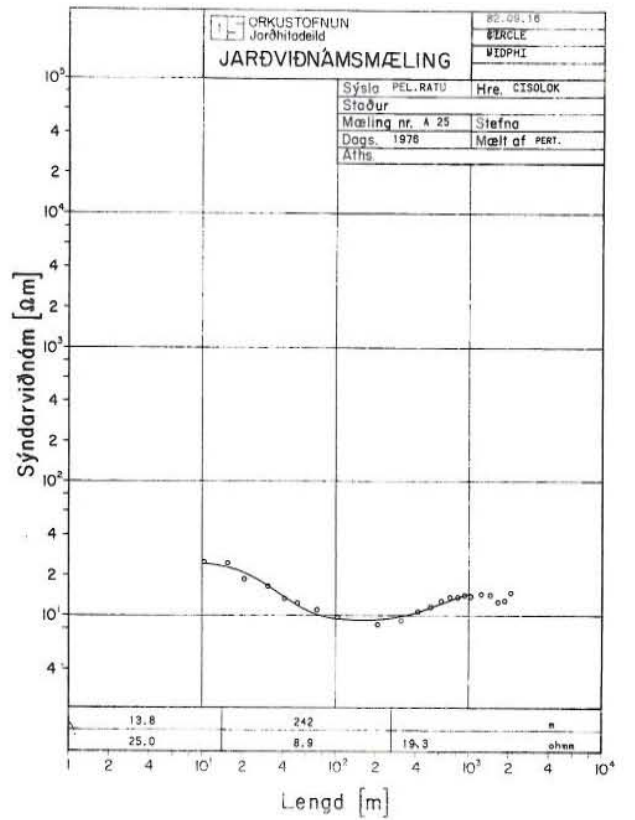
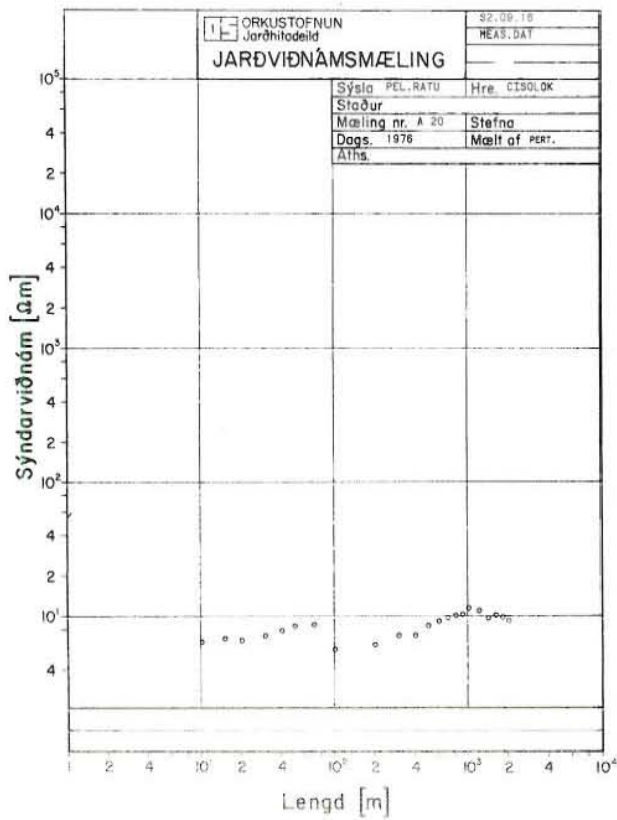
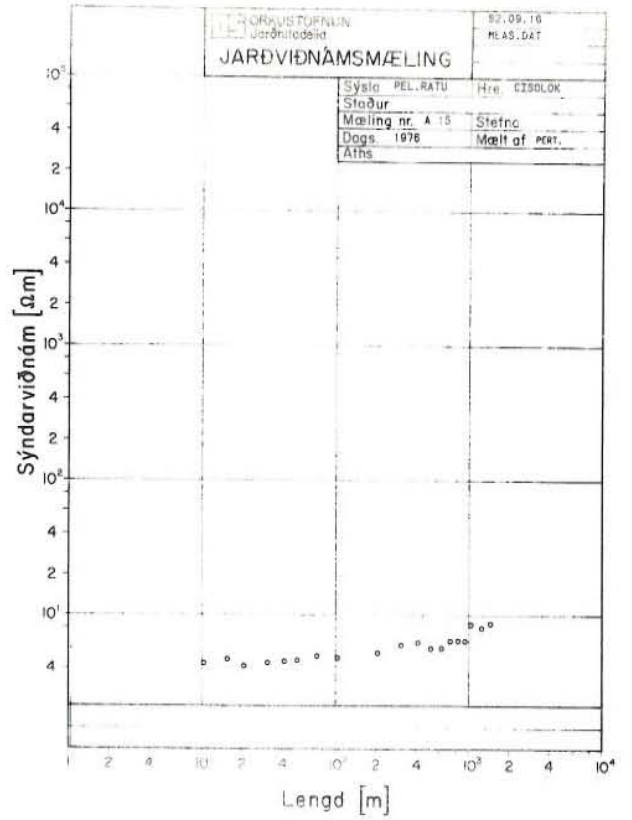
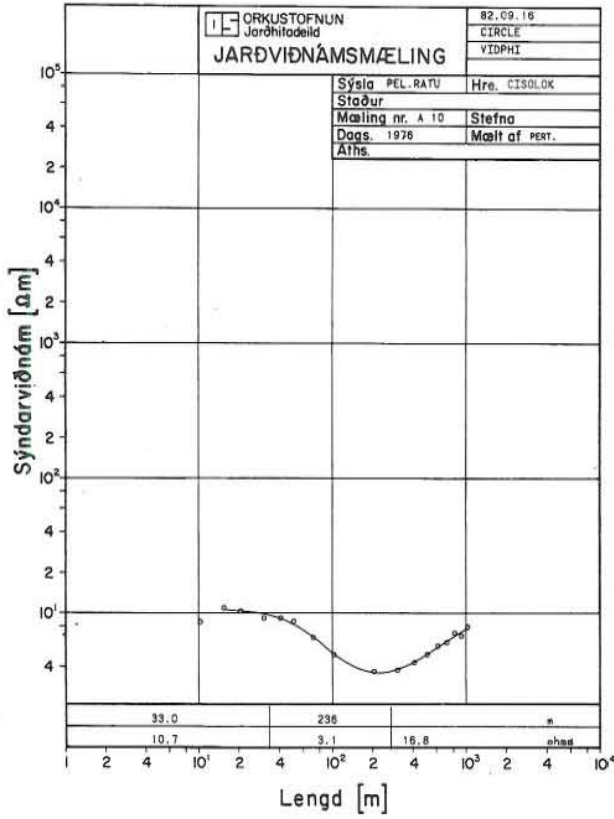
Lastly I would like to acknowledge to PERTAMINA Management especially to Dr. Joedo Sumbono, President Director of PERTAMINA, for the opportunity given to the author to attend the training course.

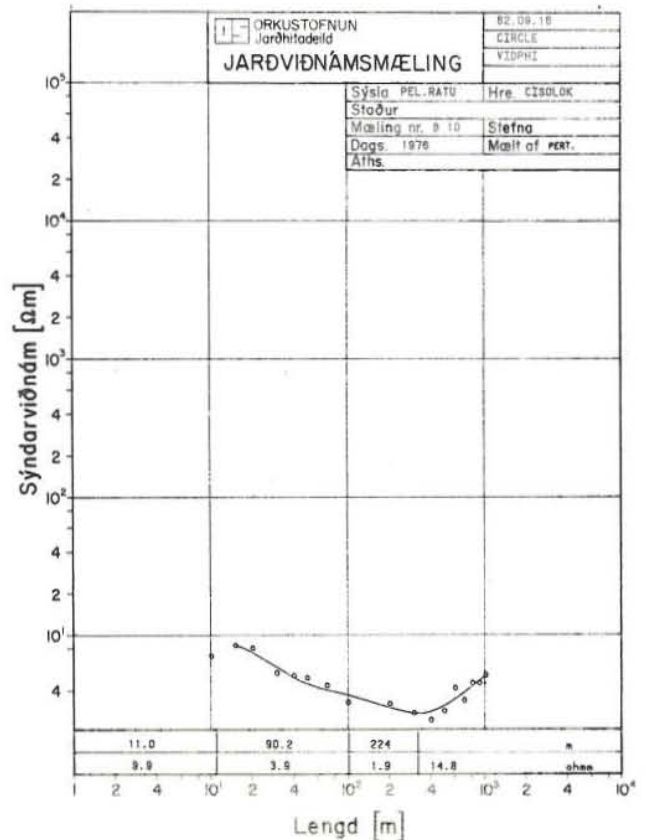
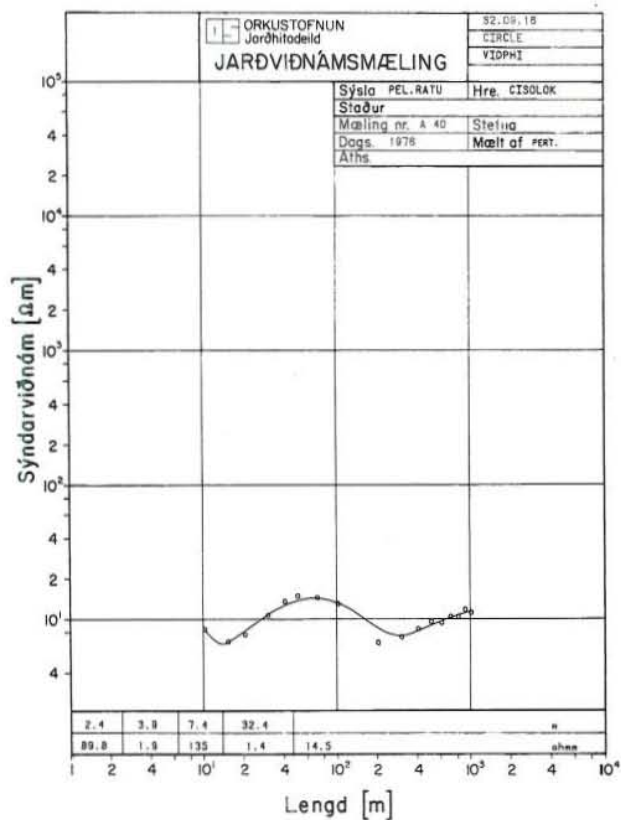
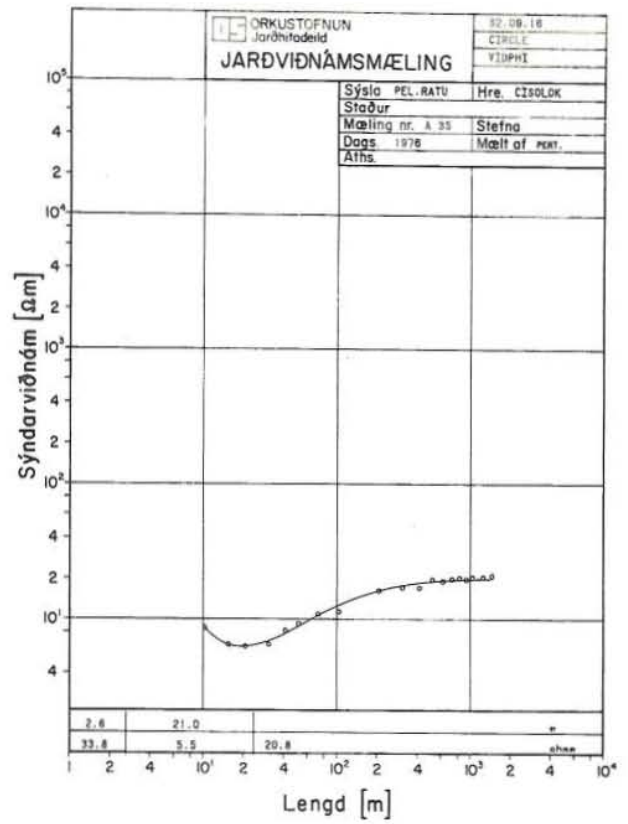
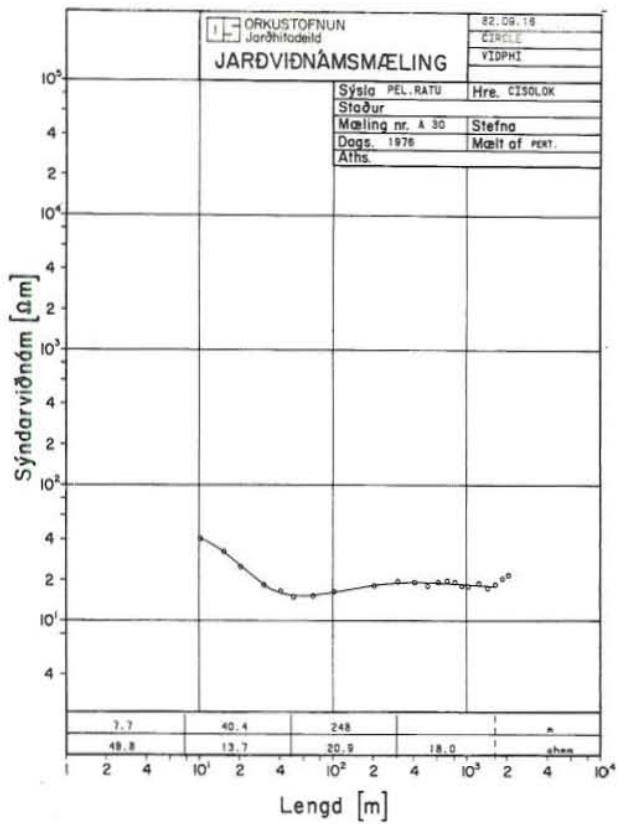
REFERENCES

- Alhamid, I. and Joko Hantono, 1982: Laporan Hasil Pengukuran Resistivity sounding Daerah Cisolok-Pelabuhan Ratu. Divisi Geothermal, Pertamina.
- Bemmelen, Van, 1949: The geology of Indonesia, Martinus Nijhoff, The Hague, Nederland, vol. IA.
- Bhattacharya, P.K. and Patra, 1968: Direct current geoelectrical sounding, Elsevier, Amsterdam, 135 pp.
- Cheng, Y.W., 1980: Location of nearsurface faults in geothermal prospects by the "combined, head-on resistivity profiling method", Proc. of the N.Z. Geothermal Workshop, 1980, 163-166.
- Dey, A. 1976: Resistivity modelling for arbitrarily shaped two-dimensional structures. Part II. User's guide to FORTRAN algorithm RESIS2D. Lawrence Berkeley Laboratory, Berkeley, LBL-5283, 56 pp.
- Dey, A and Morrison, H.F. 1976: Resistivity modelling for arbitrarily two-dimensional structures. Part I. Theoretical formulation. Lawrence Berkeley Laboratory, Berkeley, LBL-5223, 18 pp.
- Duprat, A., 1971: Geophysics in geothermal exploration, a paper published in "Annales des Mines", Paris.
- Flovenz, O. and Georgsson, L.S., 1982: Prospecting for near vertical aquifers in low temperature geothermal areas in Iceland, G.R.C. Transactions, v. 6, (in press).
- Fridleifsson, I.B., 1979: Geothermal activity in Iceland, Jokull, vol. 29, 47-56.

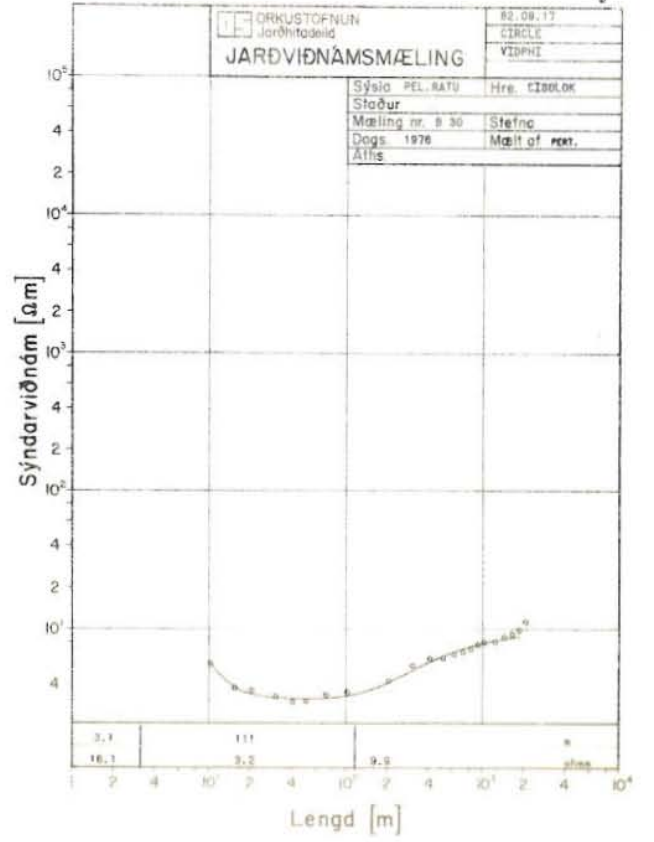
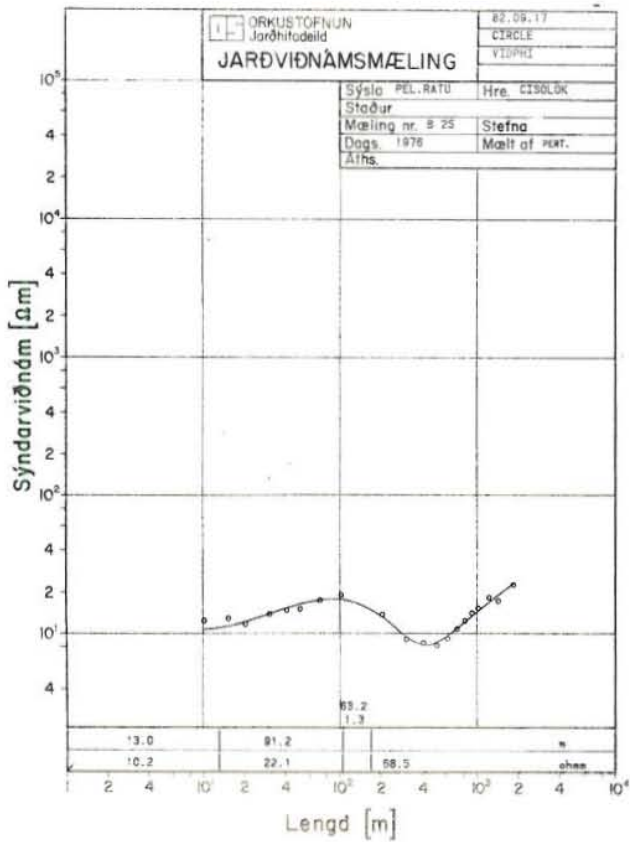
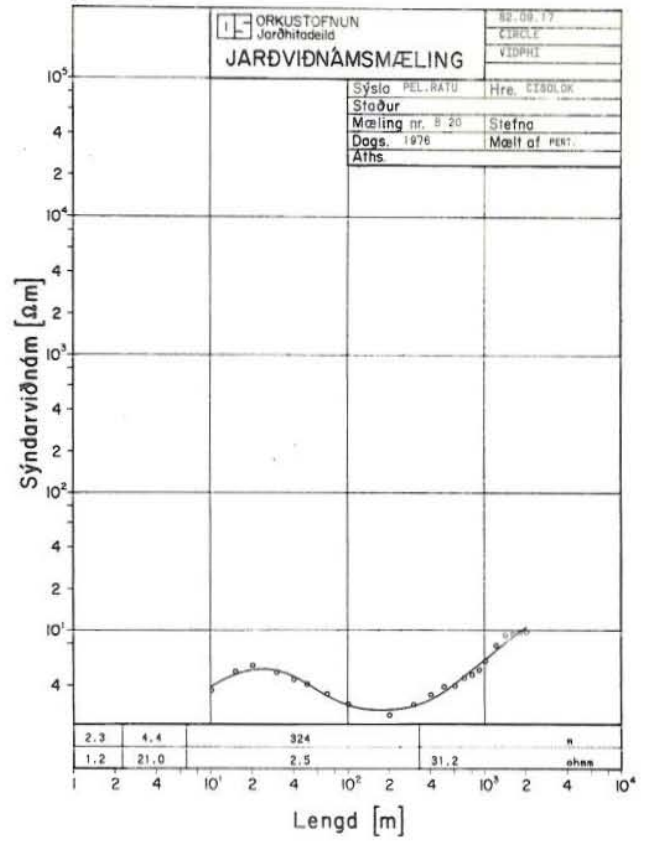
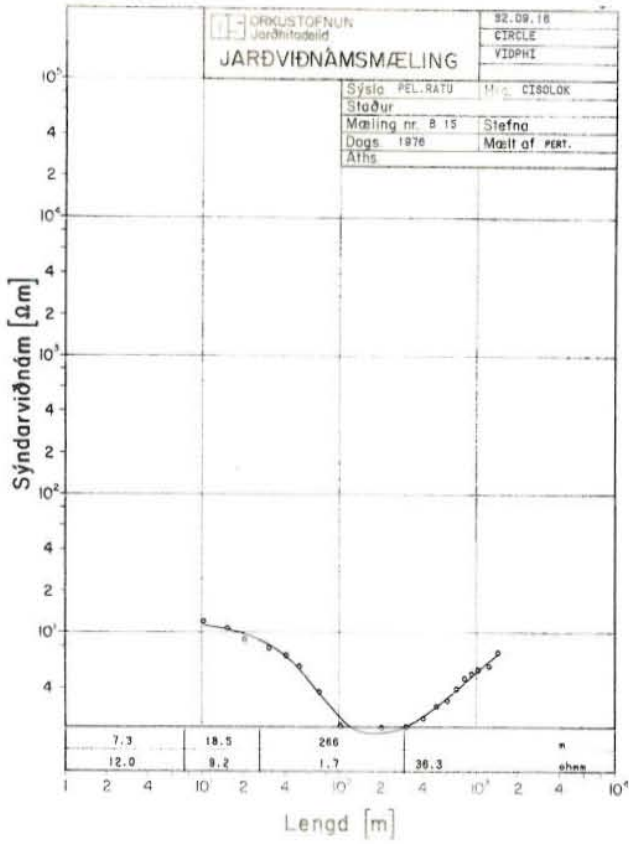
- Georgsson, L.S., 1981: A resistivity survey on the Plate Boundaries in the Western Reykjanes Peninsula, Iceland, Geothermal Resources Council, Transactions, vol. 5.
- Johansen, H.K., 1977: A man/computer interpretation system for resistivity soundings over a horizontally stratified earth, Geophys. Prosp., v. 25, 667-691.
- Keller, G.V. and Frischknecht, F. C., 1966: Electrical methods in geophysical prospecting, Pergamon Press, New York, 519 pp.
- Koefod, O., 1979: Geosounding principle 1 - Resistivity sounding measurement, Elsevier, Amsterdam, 276 pp.
- Meidav, T., 1980: DC resistivity methods in geothermal exploration in geophysical exploration method for geothermal resources, G.R.C., techn. training course no. 28b.
- Onodera, Seibe, 1976: Geophysical exploration for geothermal field. a text for the Seventh International Group Training Course on Geothermal Energy held at Kyushu University, 225 pp.
- Palmason, G., 1975: Geophysical methods in geothermal exploration, Second UN Geothermal Symposium Proc., (Lawrence Berkeley Lab., Univ. Calif.), 2173-2180.
- Rey, K. Waterstaat, The Nederlands, 1968: Standard graphs for resistivity prospecting.
- West Japan Engineering Consultants, Inc., 1976: Reports on Cisolok geothermal survey, Unpublished report, Part I, Part II.

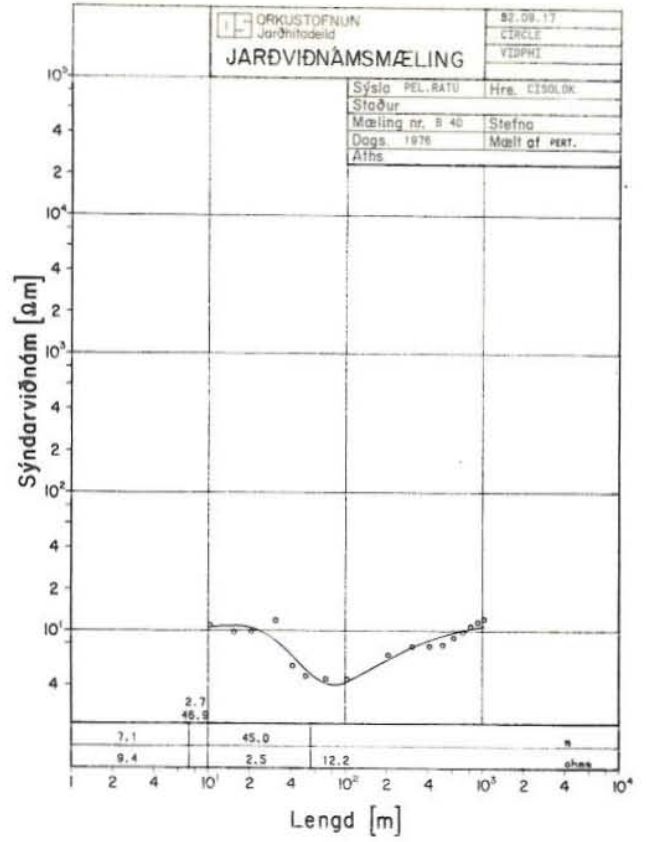
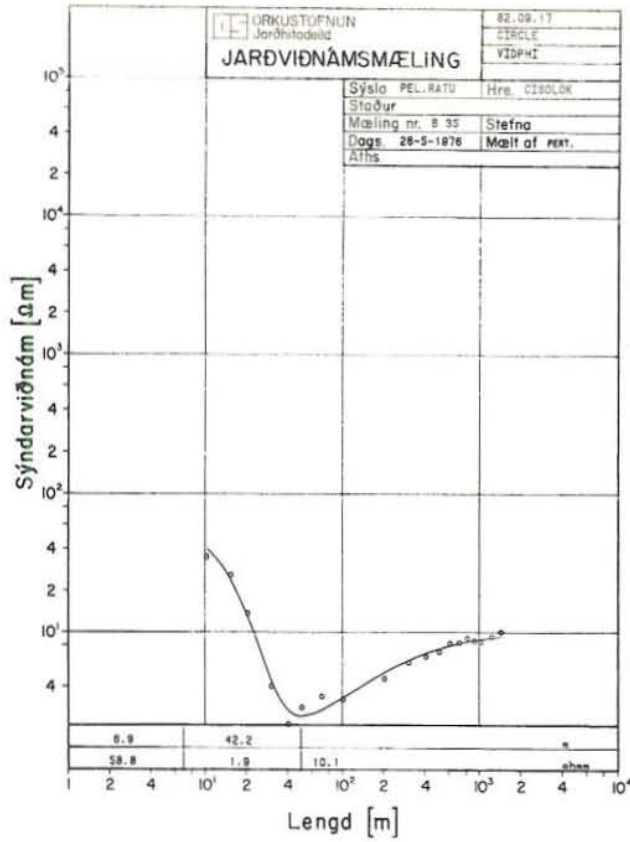
*ferna*



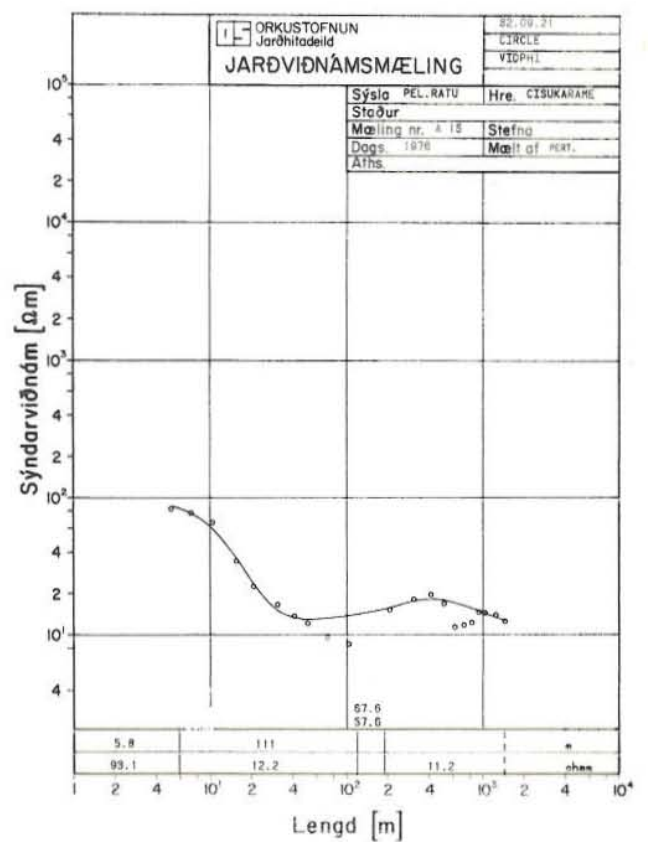
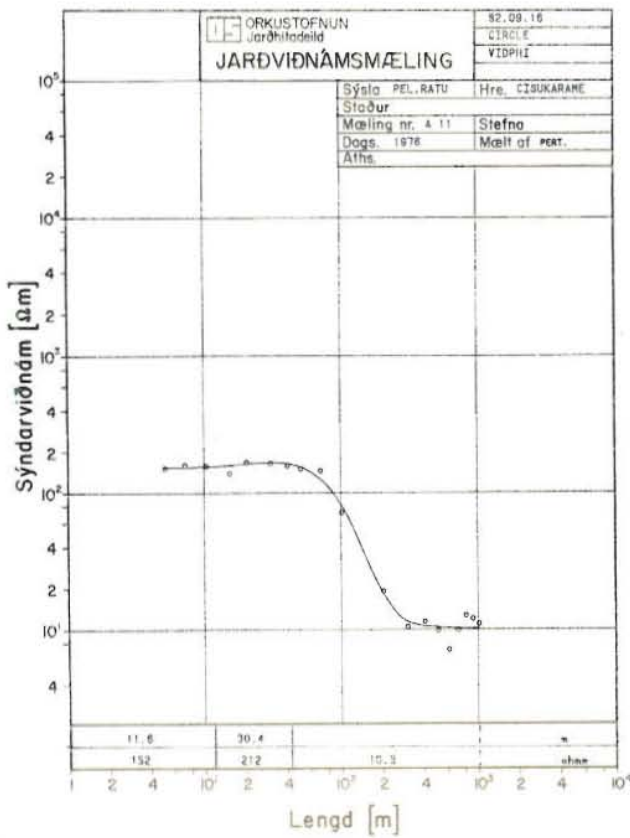


*Jörn*



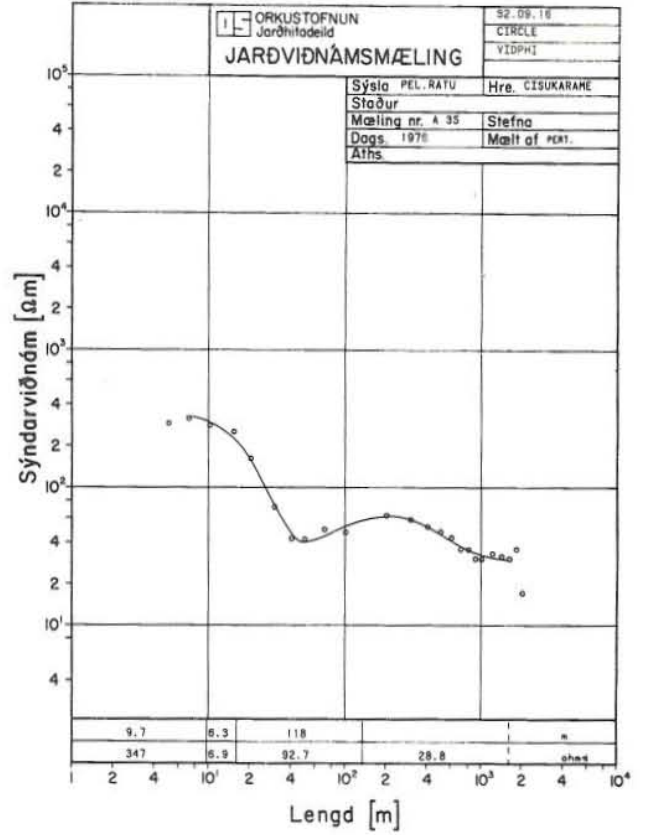
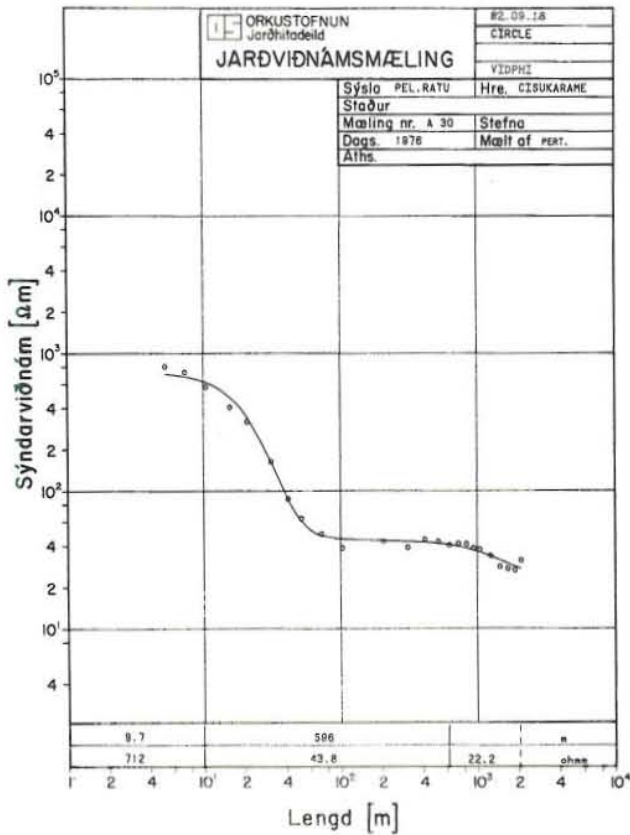
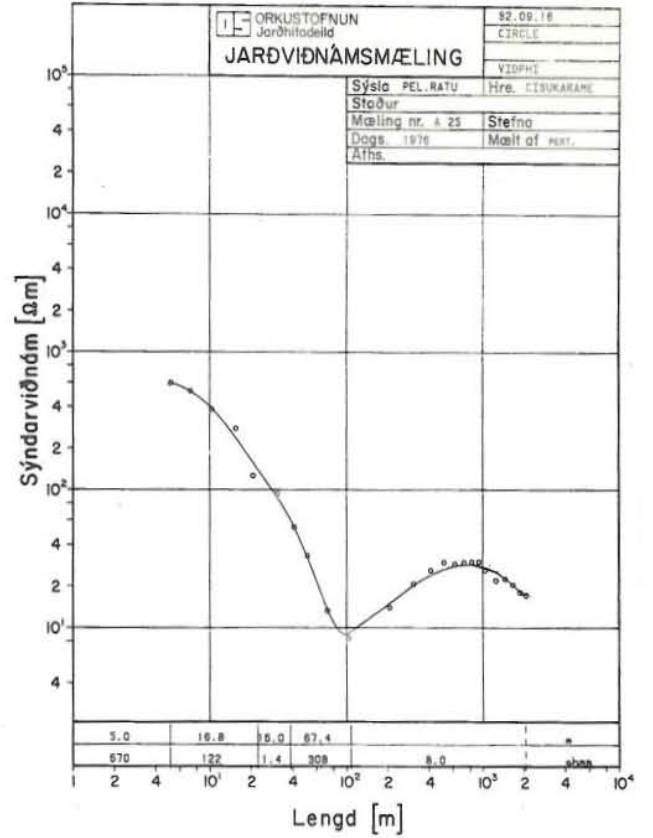
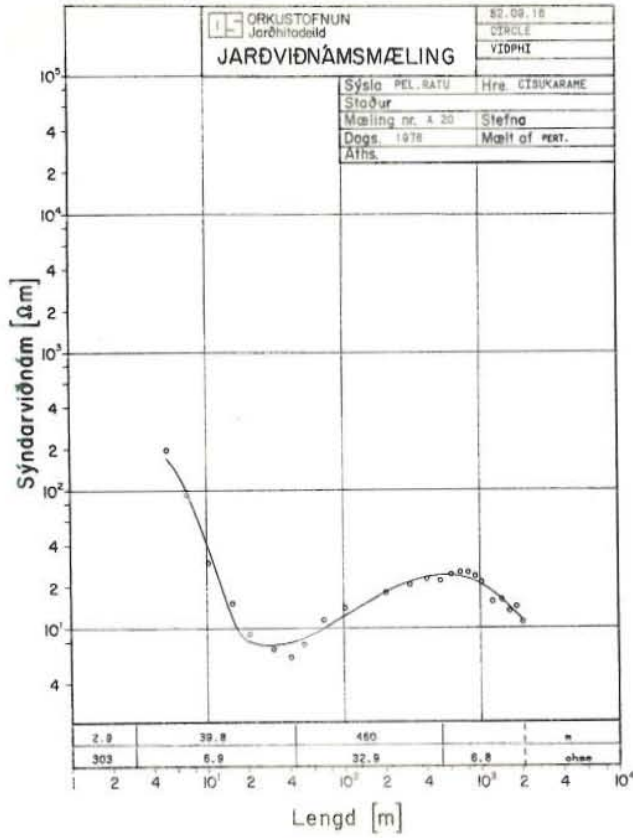


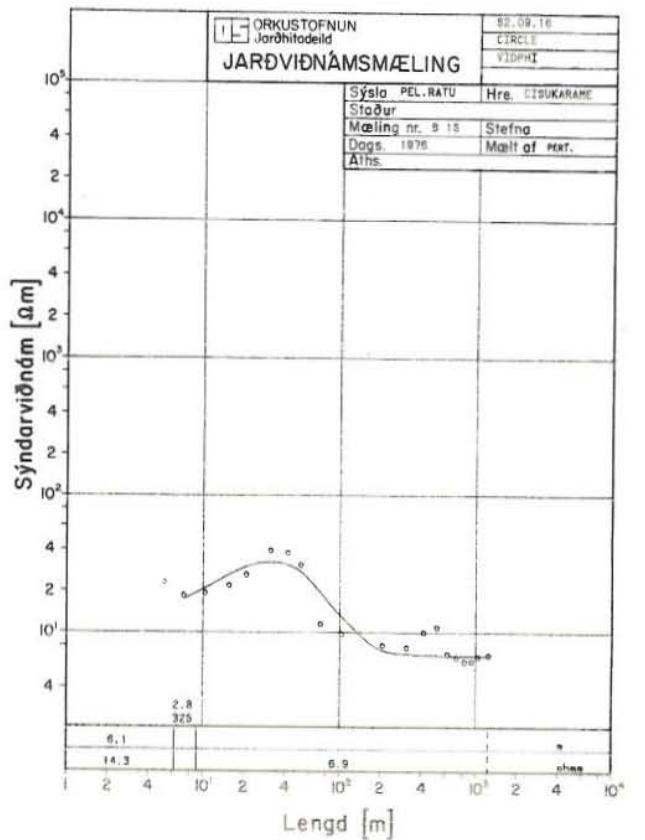
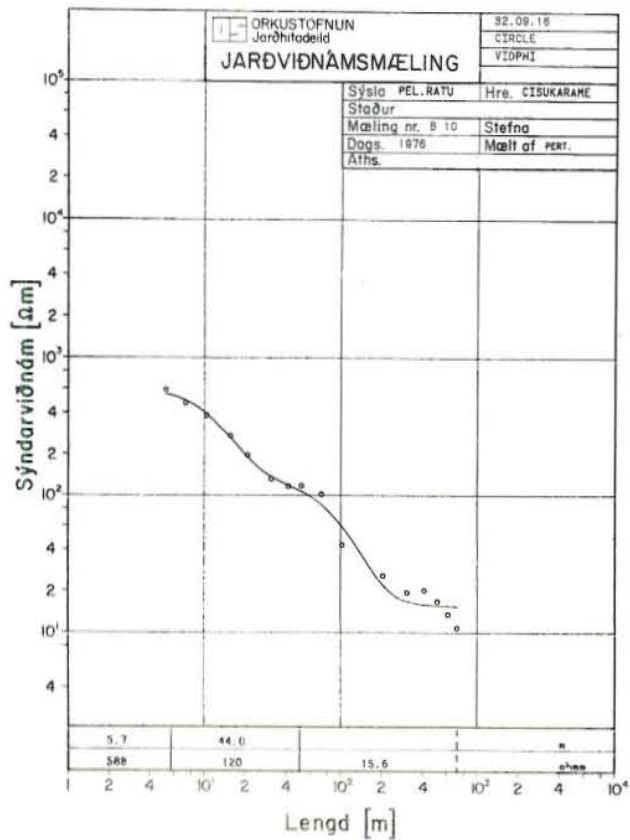
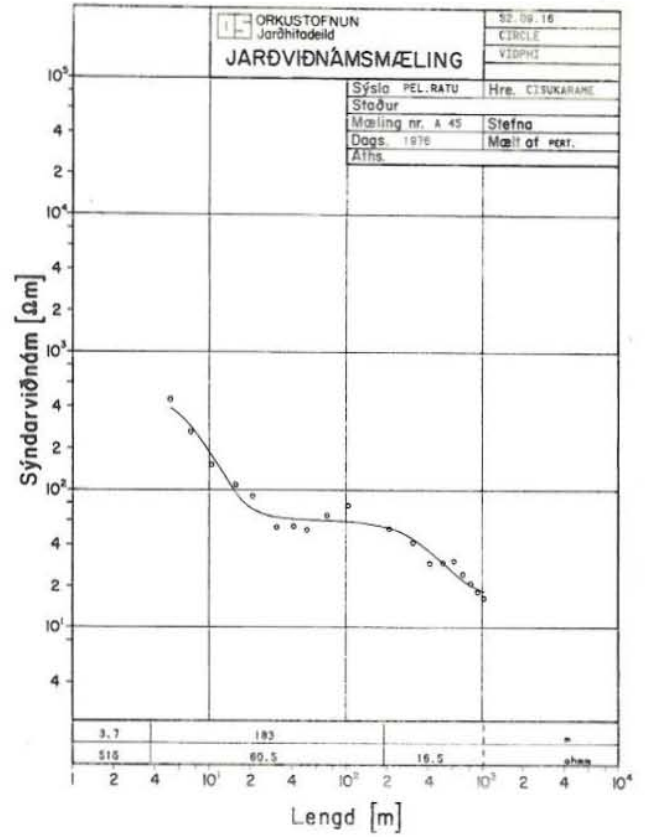
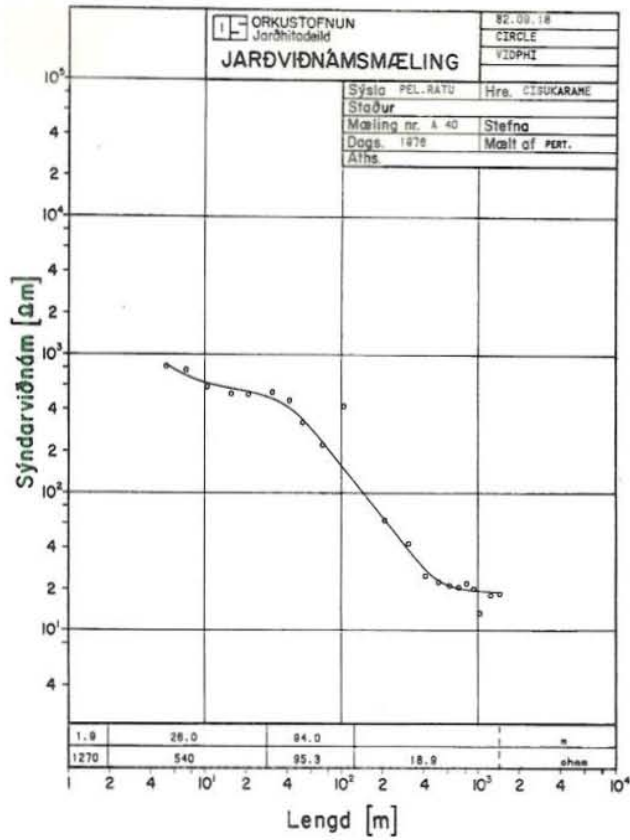
CISUKARAME



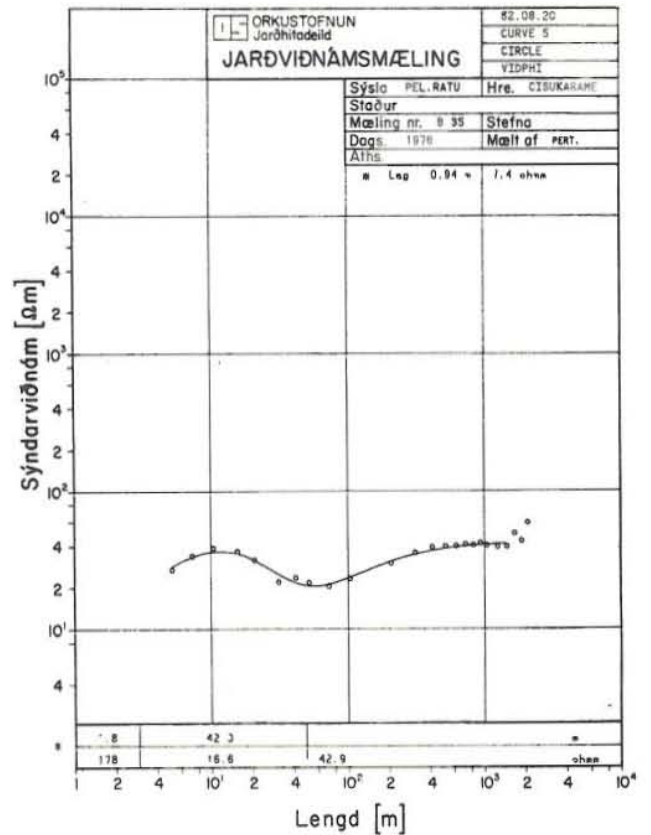
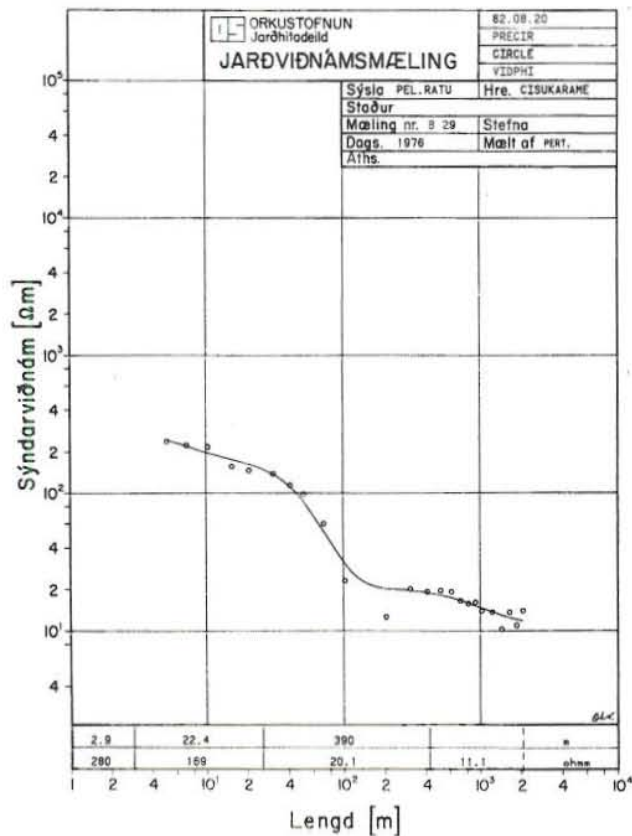
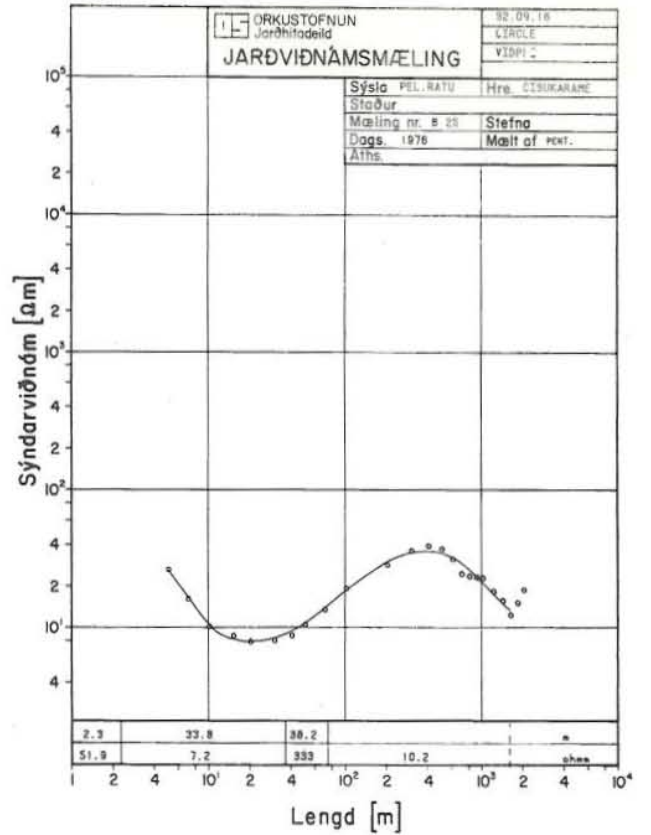
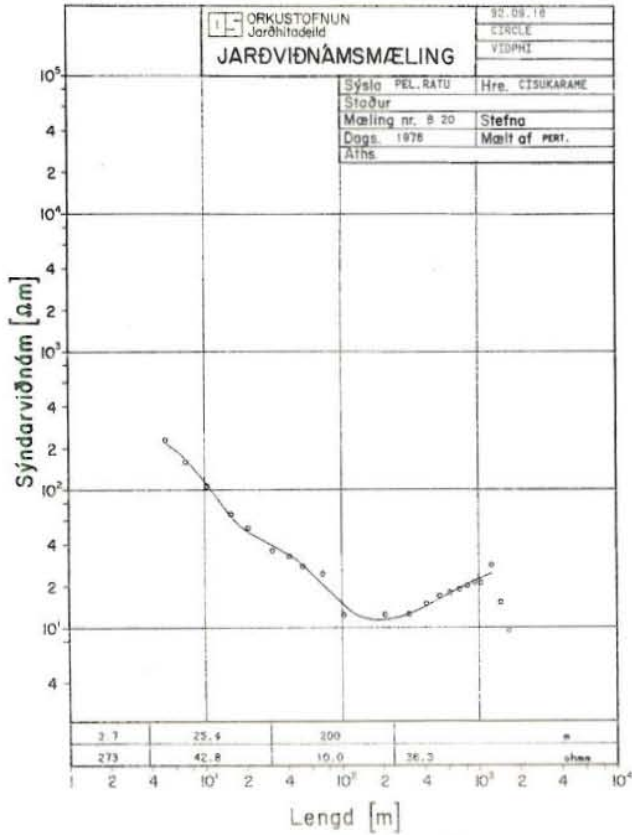


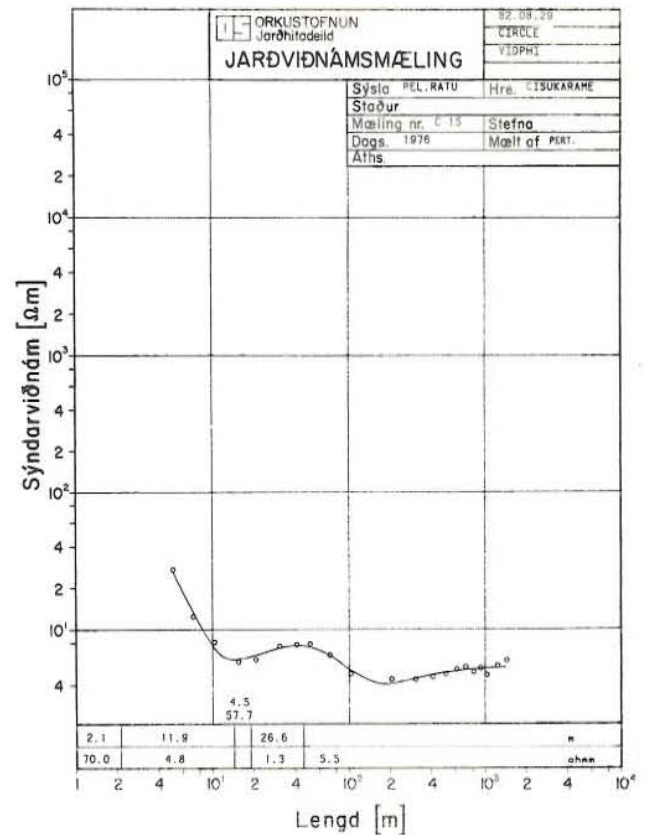
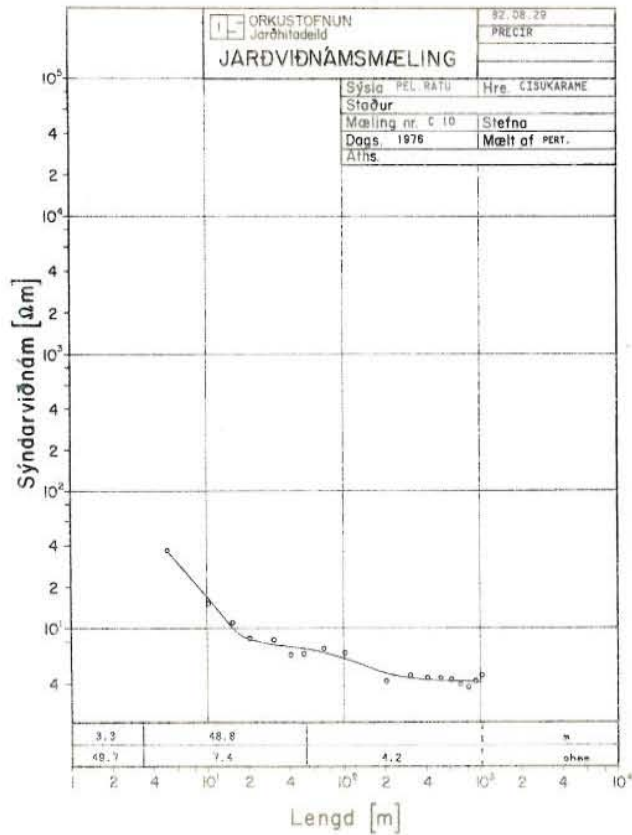
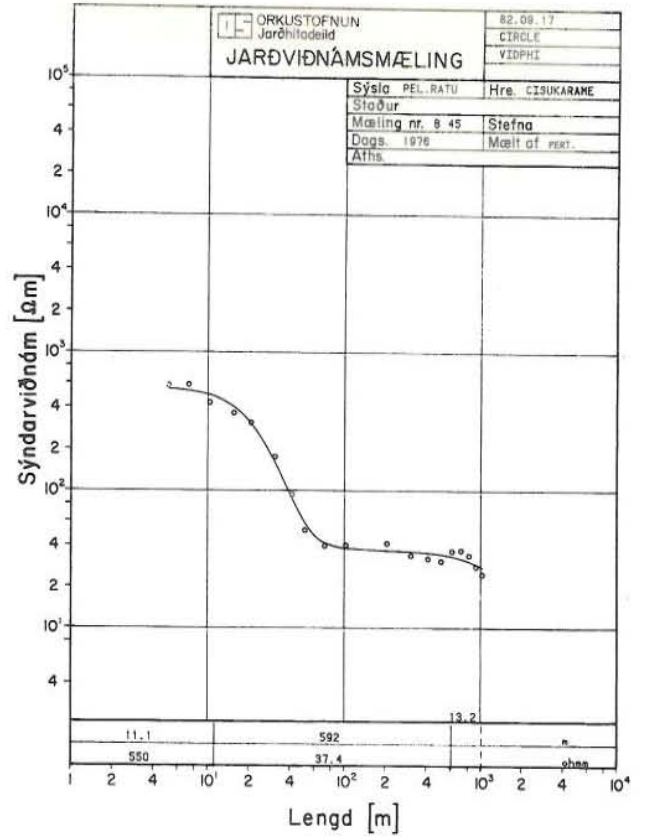
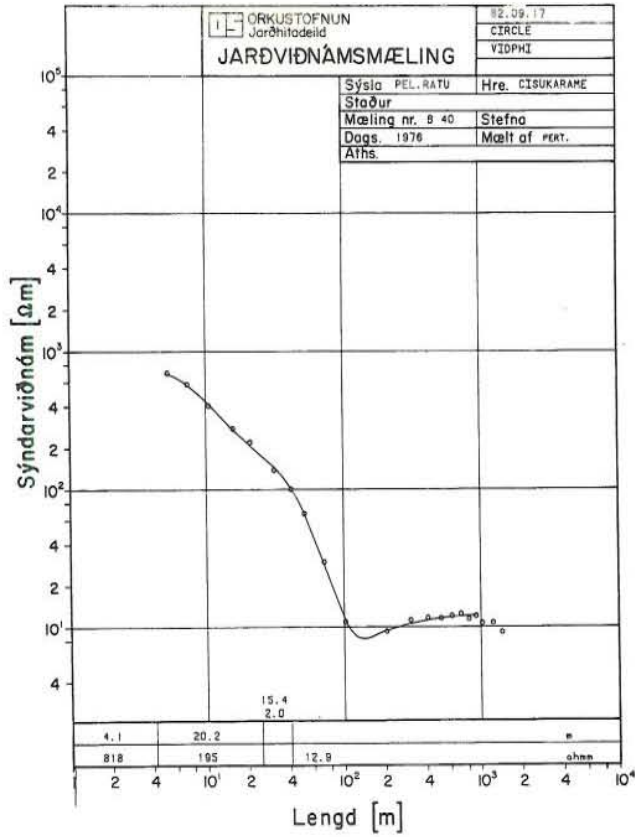
*Handwritten signature*



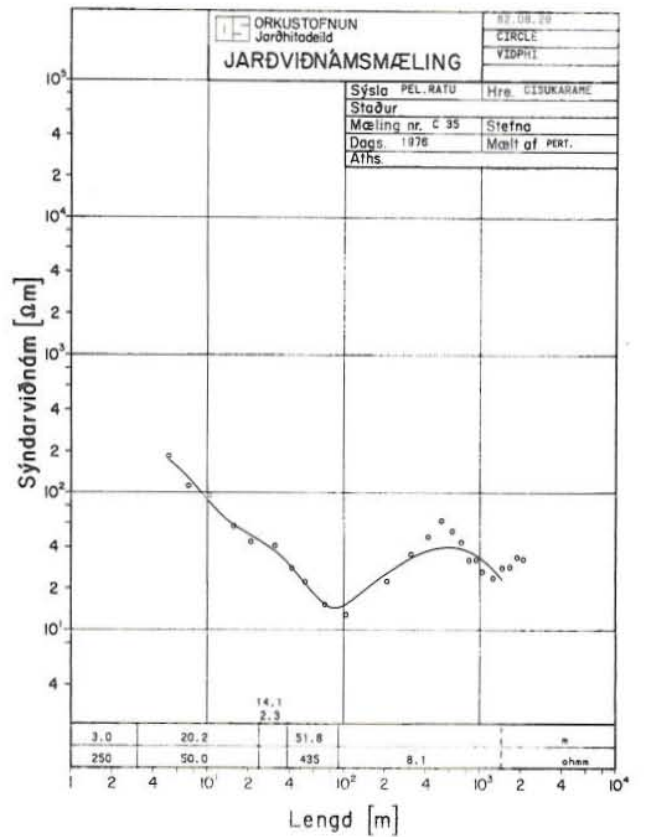
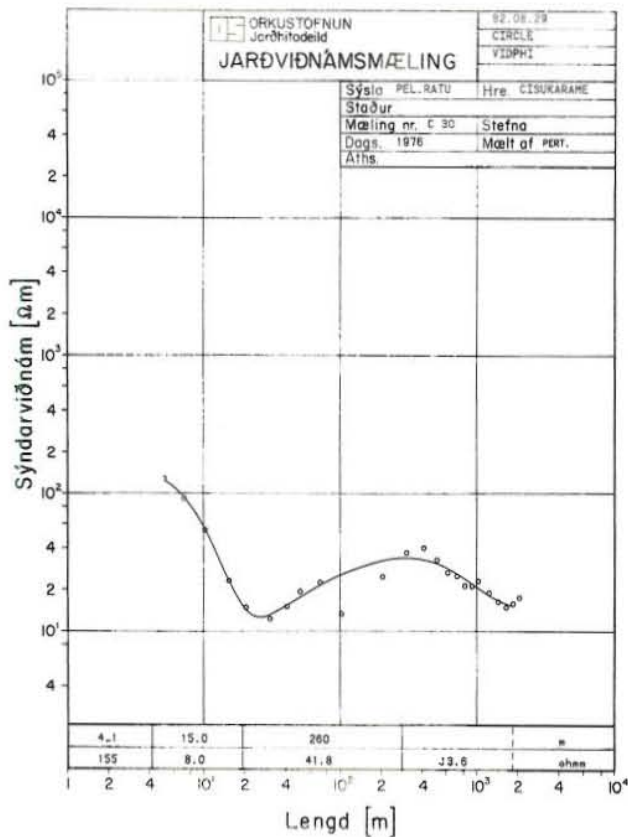
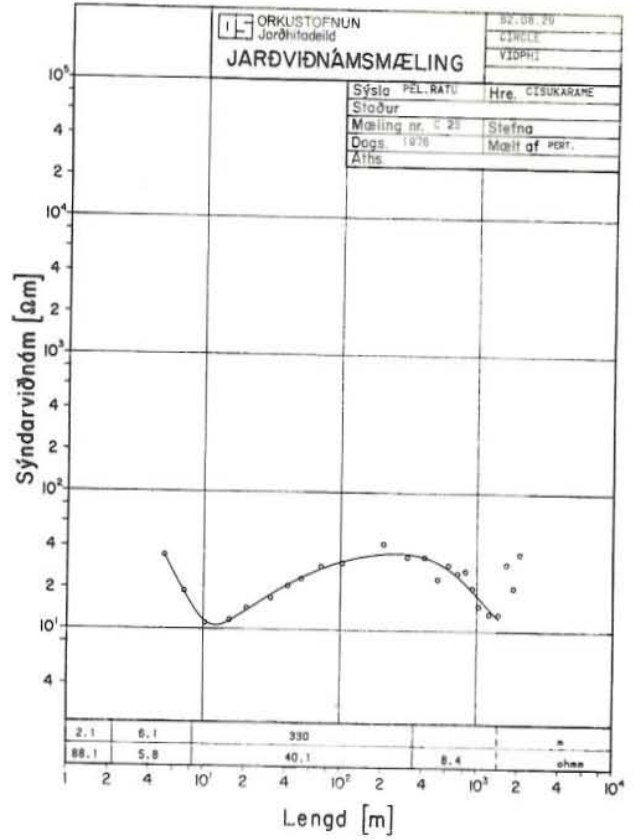
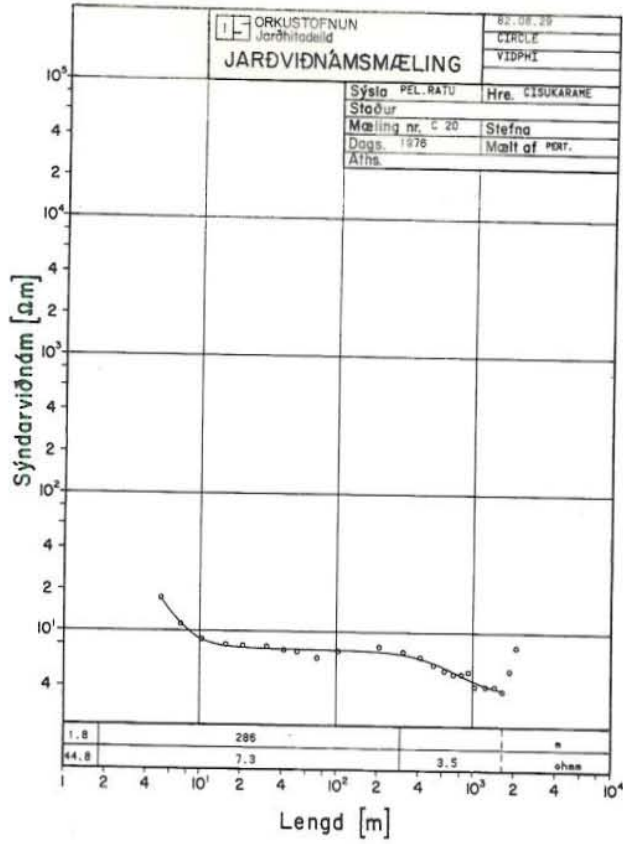


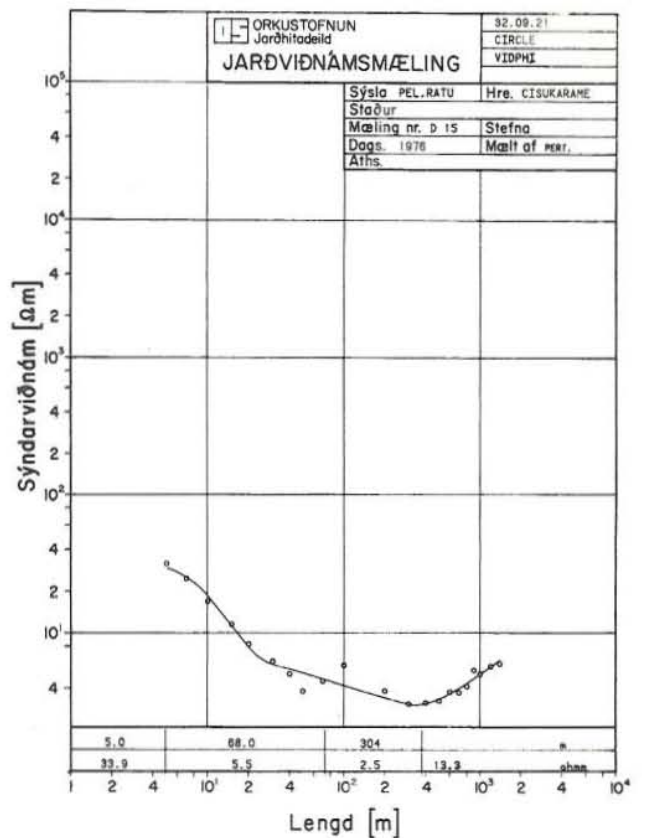
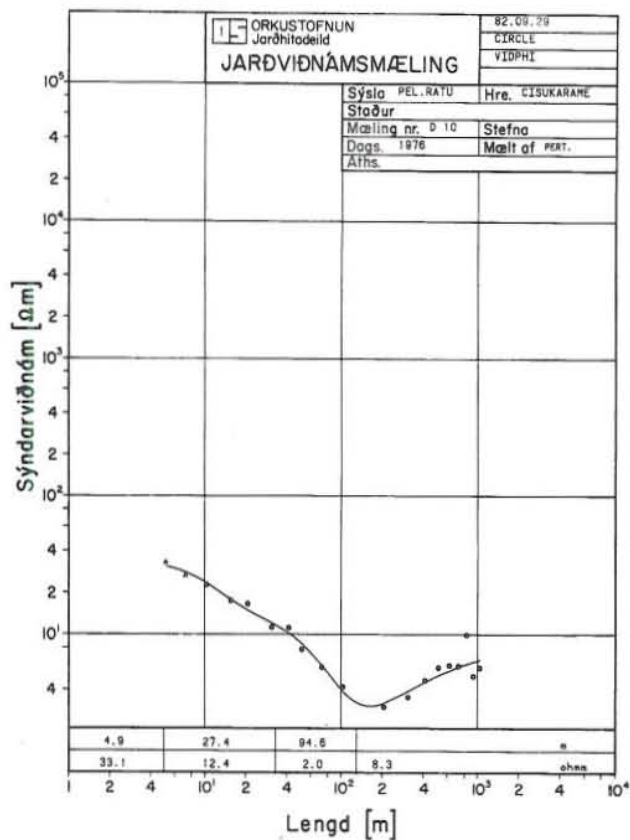
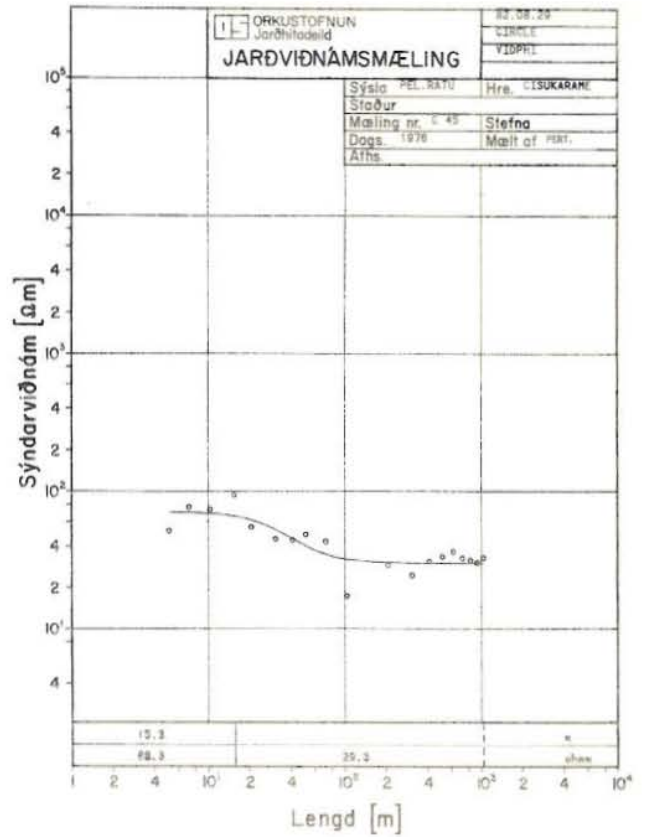
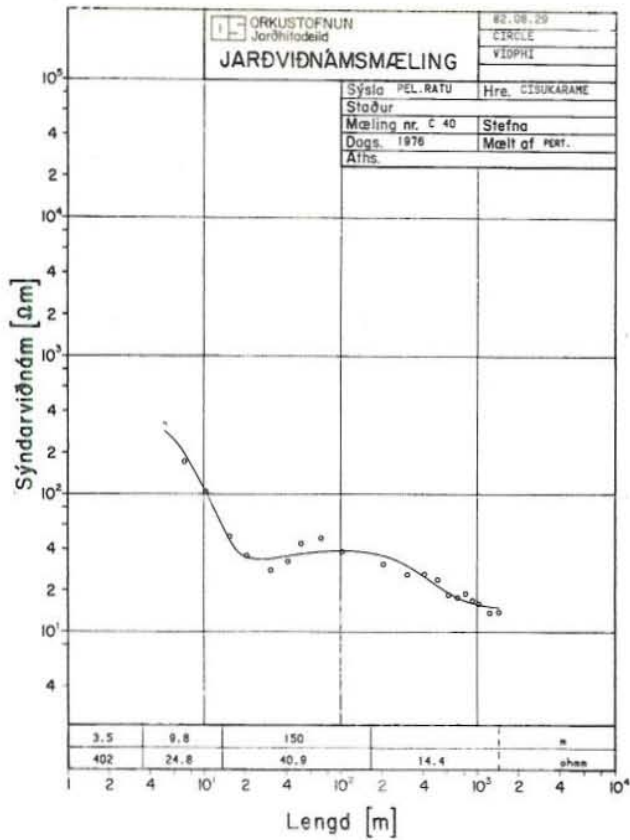
*C. J. J.*



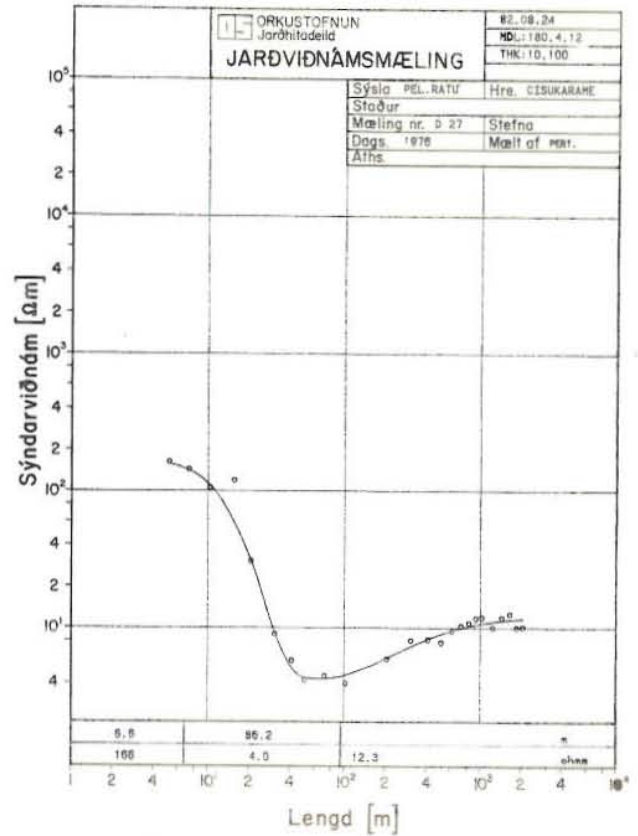
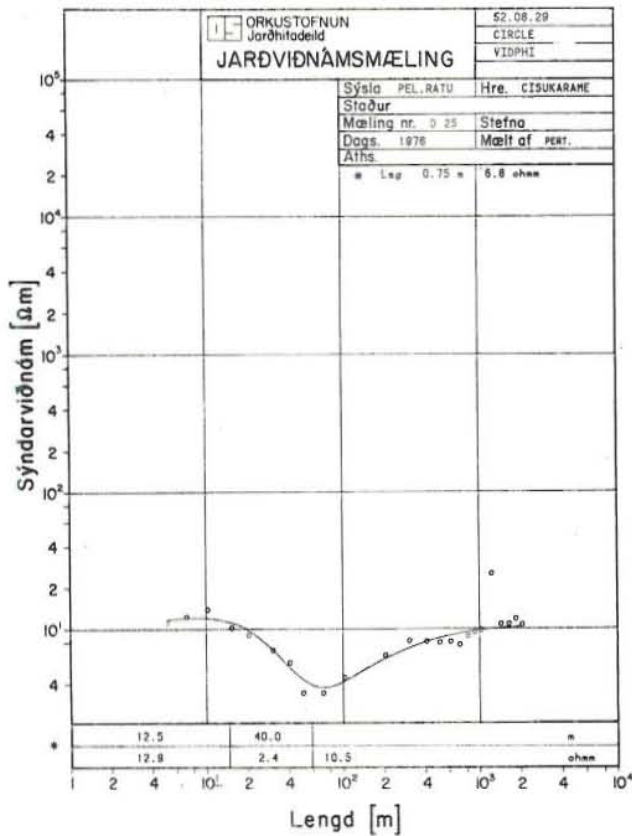
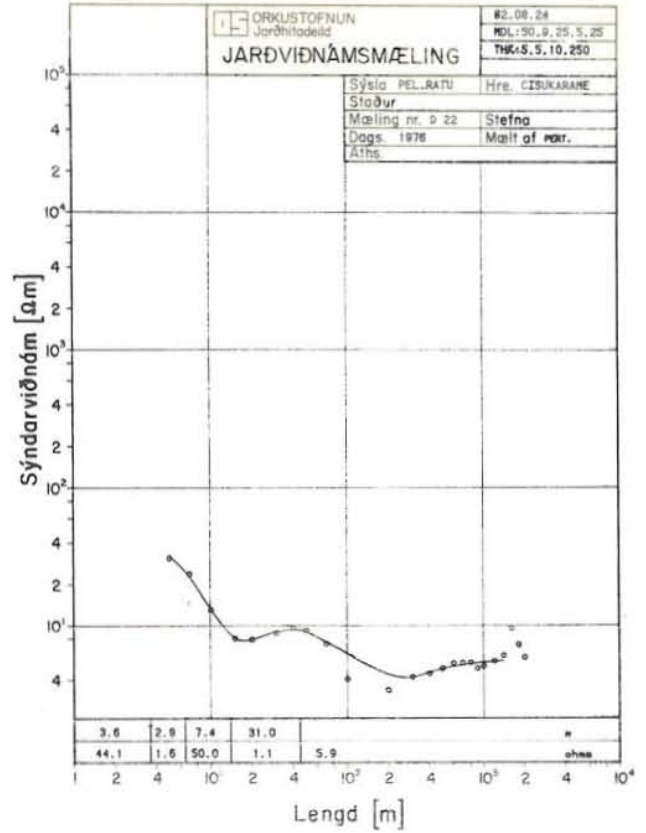
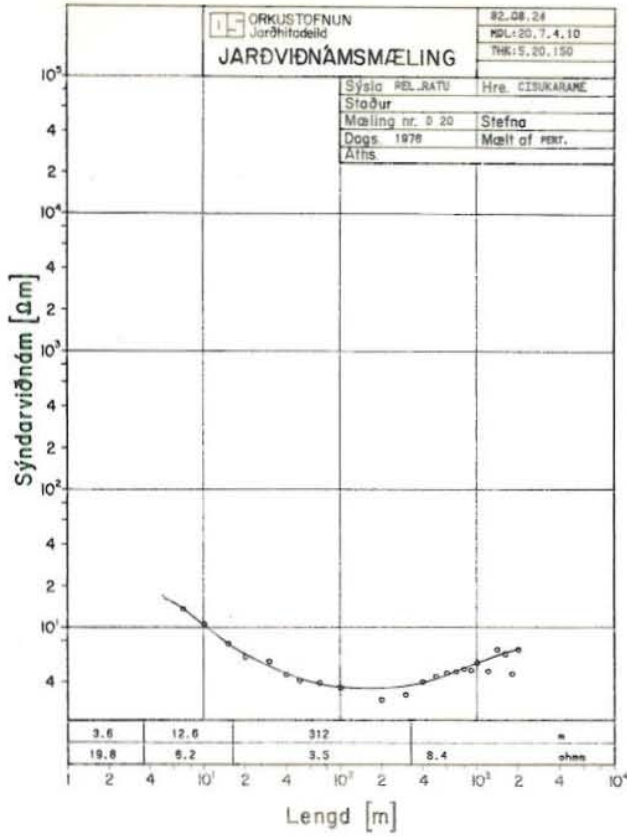


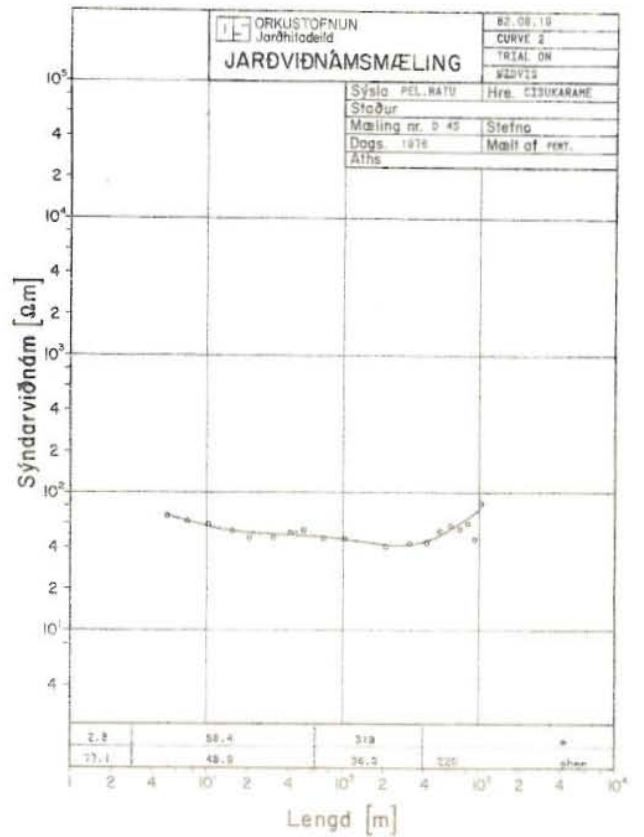
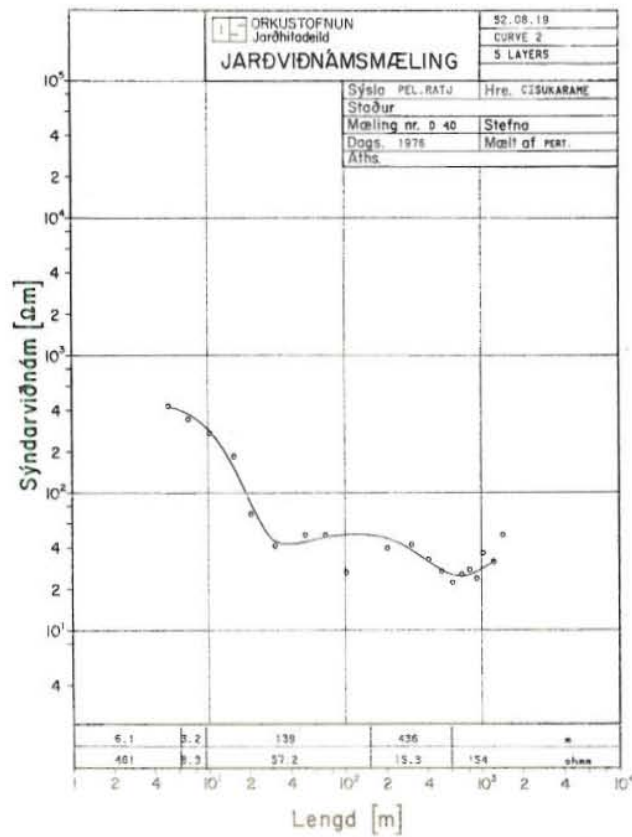
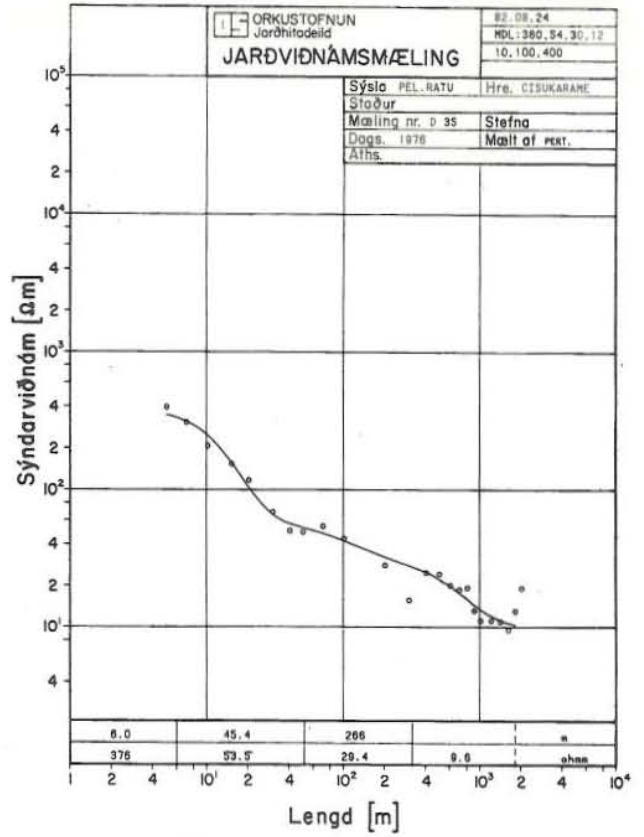
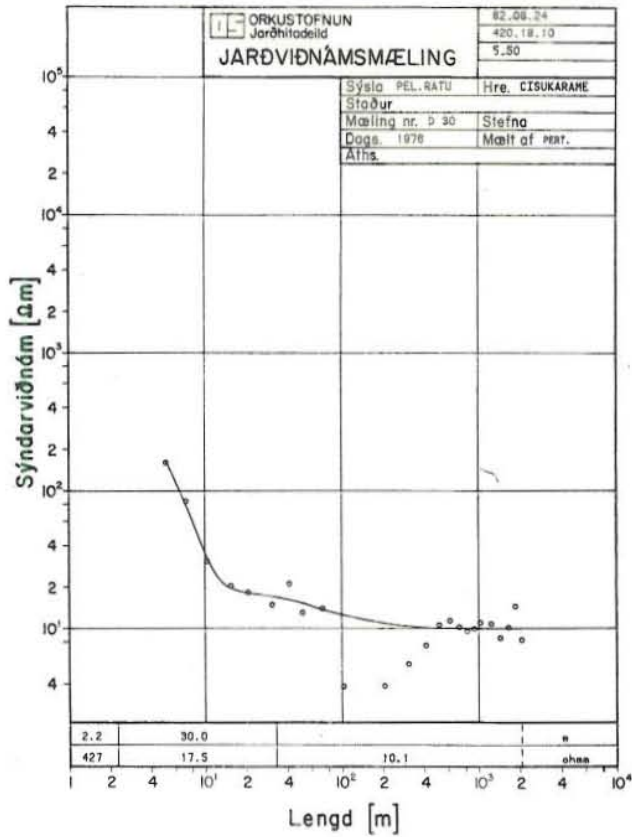
*Handwritten signature*





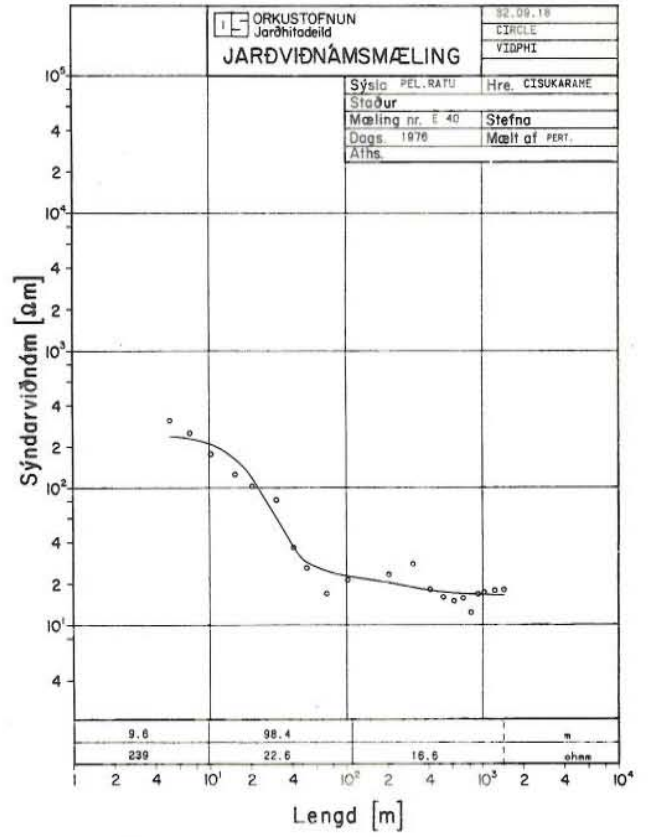
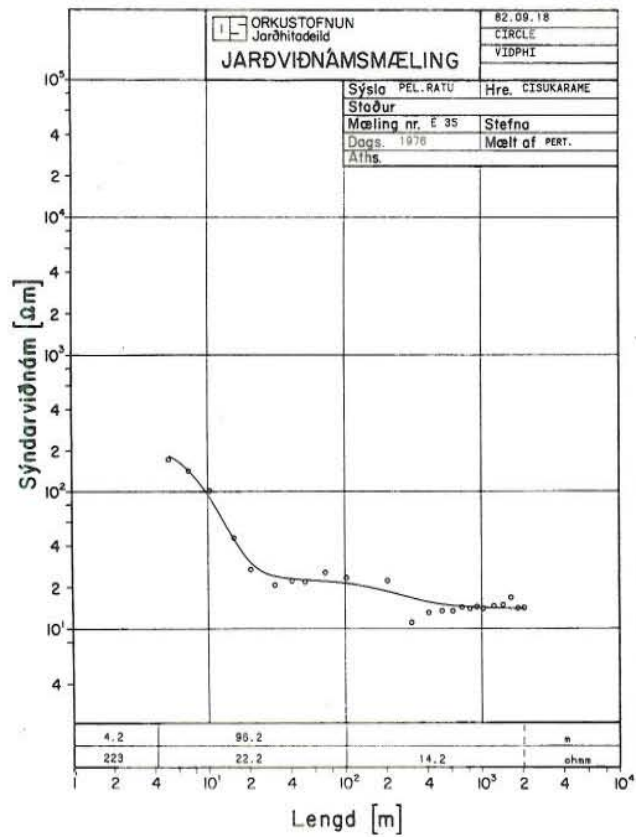
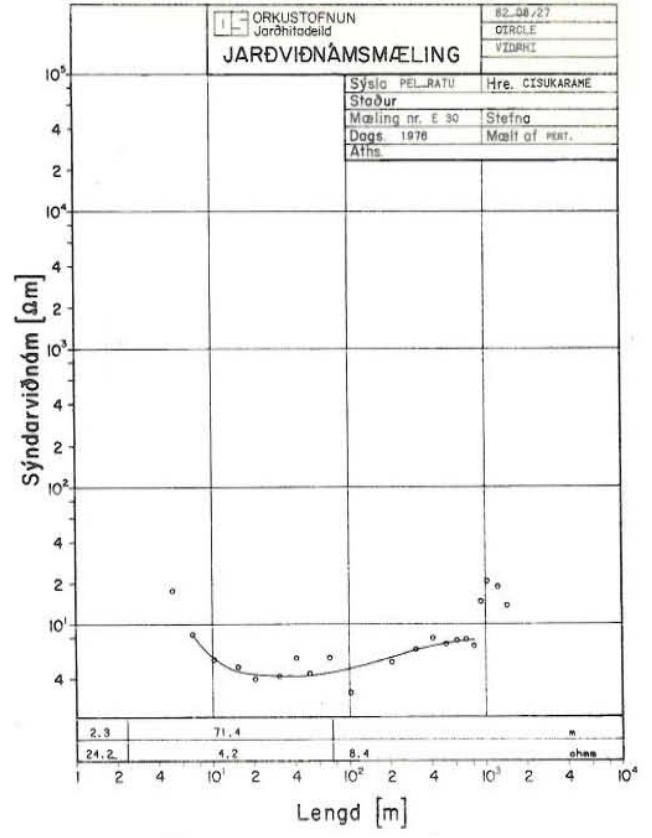
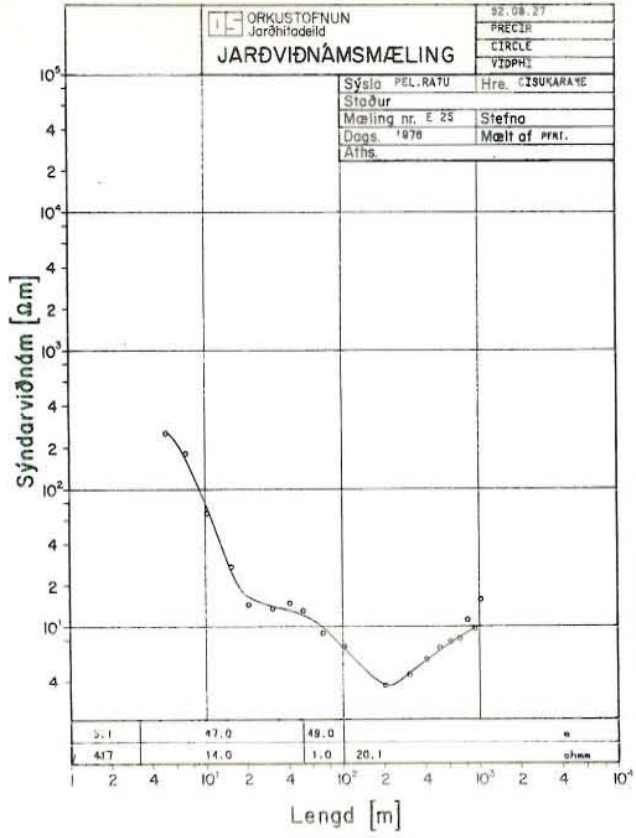
*Jan*

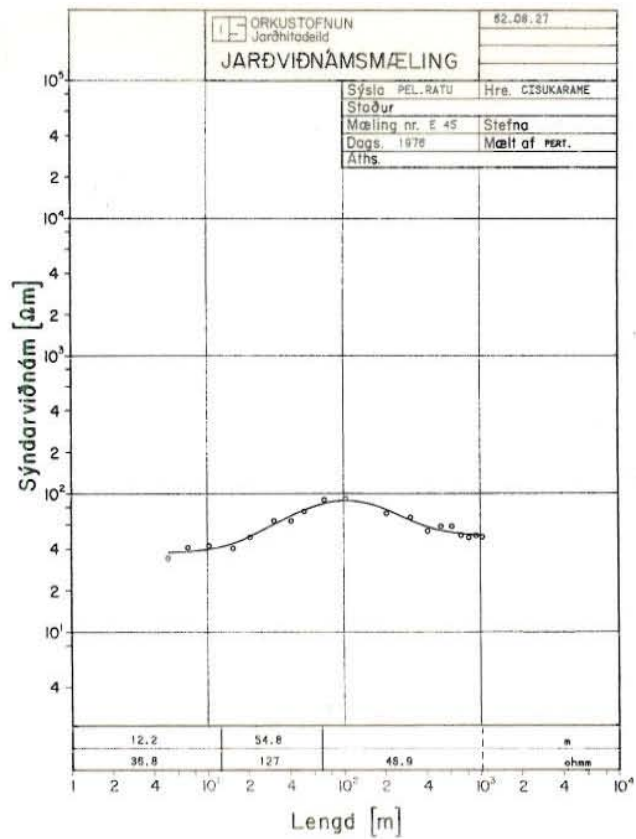






*Handwritten signature*





HITAVEITA REYKJAVIKUR  
1982-09-22

CALCULATED GEOTHERMOMETERS, SAMPLES FROM CISOLOK

SAMPLE	L/SEC	TMEAS	T CH	T QZ	T QZ	T	T A	T B	T NAK	T NAKCA		T CO2 CORR.		T NAKCAMG	
										4/3	1/3	4/3	1/3	4/3	1/3
0001	0.	71.	108.	136.	132.	16.	85.	37.	108.	100.	134.	52.	77.	100.	118.
0002	0.	89.	113.	142.	136.	21.	91.	42.	108.	99.	133.	36.	59.	99.	124.
0003	0.	95.	131.	159.	151.	37.	109.	59.	107.	117.	138.	65.	81.	117.	122.
0004	0.	96.	121.	149.	142.	27.	98.	49.	105.	112.	136.	61.	79.	112.	113.
0005	0.	75.	112.	140.	135.	19.	89.	41.	106.	93.	131.	33.	58.	93.	121.
0006	0.	83.	111.	139.	135.	19.	89.	40.	107.	99.	133.	41.	65.	99.	114.
0007	0.	80.	113.	142.	136.	21.	91.	42.	106.	95.	131.	42.	68.	95.	114.
0008	0.	93.	121.	149.	142.	27.	98.	49.	105.	106.	134.	57.	78.	106.	112.
0009	0.	96.	118.	146.	140.	25.	95.	46.	106.	105.	134.	59.	81.	105.	115.
0010	0.	97.	119.	147.	141.	25.	96.	47.	104.	103.	133.	51.	73.	103.	111.
0011	0.	82.	122.	150.	143.	28.	99.	50.	105.	97.	132.	37.	61.	97.	111.
0012	0.	70.	115.	143.	138.	22.	93.	44.	115.	69.	127.	15.	56.	999.	999.
0013	0.	86.	123.	151.	144.	29.	100.	51.	107.	97.	132.	34.	58.	97.	111.
0014	0.	83.	118.	146.	140.	25.	95.	46.	108.	96.	132.	40.	65.	96.	112.
0015	0.	55.	113.	142.	136.	21.	91.	42.	103.	87.	128.	999.	999.	87.	111.
0016	0.	87.	116.	144.	138.	23.	93.	44.	107.	95.	132.	37.	63.	95.	112.
0017	0.	89.	132.	159.	151.	37.	109.	60.	106.	99.	132.	40.	63.	99.	114.
0018	0.	88.	108.	137.	132.	16.	86.	37.	107.	93.	131.	45.	74.	93.	121.
0019	0.	62.	97.	125.	122.	6.	74.	26.	117.	80.	132.	29.	66.	80.	83.
0020	0.	88.	120.	148.	141.	26.	97.	48.	107.	101.	134.	50.	74.	101.	115.
0021	0.	63.	122.	150.	143.	29.	100.	51.	104.	95.	130.	999.	999.	95.	116.
0022	0.	86.	119.	147.	141.	25.	96.	47.	105.	96.	131.	38.	63.	96.	116.
0023	0.	69.	124.	152.	145.	30.	101.	52.	105.	102.	133.	41.	62.	102.	124.
0025	0.	96.	119.	147.	141.	26.	97.	48.	106.	99.	133.	46.	71.	99.	115.

HITAVEITA REYKJAVIKUR  
1982-09-22

CALCULATED GEOTHERMOMETES, SAMPLES FROM CISUKARAME

SAMPLE	L/SEC	TMEAS	T CH	T QZ	T QZ	T	T A	T B	T NAK	T NAKCA		T CO2 CORR.		T NAKCAMG	
										4/3	1/3	4/3	1/3	4/3	1/3
0001	0.	98.	148.	175.	164.	52.	125.	75.	163.	220.	191.	999.	999.	220.	191.
0002	0.	93.	65.	94.	96.	0.	44.	-3.	263.	44.	171.	6.	98.	999.	999.
0003	0.	75.	110.	138.	134.	18.	88.	39.	167.	136.	171.	70.	95.	120.	128.
0004	0.	98.	139.	166.	157.	43.	116.	66.	165.	155.	176.	79.	93.	164.	165.
0005	0.	93.	140.	168.	158.	45.	117.	68.	164.	155.	176.	70.	83.	152.	162.
0006	0.	85.	127.	155.	148.	33.	105.	55.	159.	132.	167.	63.	87.	132.	165.